An Incremental Shifting Vector Approach for Reliability-Based Design Optimization

Z.L. Huang [a], C. Jiang [*a], Y.S. Zhou [a], Z. Luo [b], Z. Zhang [a]

[a] *State Key Laboratory of Advanced Design and Manufacturing for Vehicle Body, College of Mechanical and Vehicle Engineering, Hunan University, Changsha City, P. R. China 410082*

[b] *School of Mechanical and Mechatronic Engineering, University of Technology, Sydney, NSW 2007, Australia*

Abstract:

This paper proposes a decoupling algorithm for reliability-based design optimization (RBDO) with high performance in terms of efficiency and convergence, which provides an effective tool for reliability design of many complex structures. The algorithm proceeds by performing a shifting vector calculation and then solving a deterministic design optimization in each step, and eventually converges to the optimal solution. An incremental shifting strategy is proposed to ensure stable convergence in the iteration process. In each step, the shifting vector preserves the information from the previous step, and only an adjustment is made for it through a shifting vector increment. A computation method is given for the shifting vector increment, avoiding solving an optimization problem during the reliability analysis and thus greatly reducing the computational cost of the iteration process. Six numerical examples and two engineering applications are presented to validate the effectiveness of the method proposed in this paper.

Keywords: Reliability-based design optimization (RBDO); incremental shifting vector; decoupling approach

[*] Corresponding author. Tel: 86-731-88823325; fax: 86-731-88821445

E-mail address: jiangc@hnu.edu.cn (Chao Jiang)

1 Introduction

There exist many uncertainties in practical engineering problems, including geometric dimensions, material properties, and loads. The combined effects of these uncertain factors can lead to large variations in the structural properties and even failure. Reliability-based design optimization (RBDO) [1-7] can fully take into account the impact of these uncertainties on the constraints in the optimization process; therefore, it can make the result satisfying the requirements of reliability and hence plays an important role in practical safety design of structures and products. RBDO has become an important research direction in the field of structural reliability, and a series of important theories and methods have been developed in this area. However, from an overall perspective, RBDO still in the developing stage, and some key issues need to be resolved, efficiency being one of them. Performing RBDO usually involves a two-layer nested optimization, with the outer layer being optimization of the design variables and the inner layer being the reliability analysis. However, practical engineering problems are generally solved using time-consuming numerical simulation techniques such as the finite element method (FEM). Thus, nested optimization based on the simulation model will lead to extremely low computational efficiency. Some important RBDO methods have been developed to address this efficiency issue, which can be roughly grouped into two categories. One category is response surface methods, which greatly reduce computational cost by constructing an analytic function to replace the time-consuming numerical simulation in the optimization process. Youn et al. [8] used a selective interaction sampling technique to construct an interpolation response surface; they combined this technique with an inverse reliability analysis technique to reduce the FEM calls, and the RBDO efficiency could be improved. Kim et al. [9] used the response surface based on the moving least squares method for reliability optimization and estimated the impact of the response surface error on the RBDO analysis results. Basudhar and Missoum [10] used the support vector machine to deal with the constraints and whereby developed an efficient probabilistic optimization design method, which also could handle the problems with discontinuous limit state functions. Shan and Wang [11] used the mode-pursuing sampling method to construct a Kriging approximation model for high-efficiency RBDO. Zhuang and Pan [12] employed a sequential expected improvement strategy for sampling and continuously refreshed the response surface during the RBDO process to ensure convergence. The above methods improved the computational efficiency of RBDO significantly. However, for many complex engineering problems, especially those with high dimensionalities and large numbers of reliability constraints, establishing a highly accurate response surface function to ensure accuracy of the RBDO computation is not an easy task.

The second category is decoupling methods [13-27]. The basic idea of this type of method is to decouple the nested optimization in RBDO into a series of iterative processes that are composed of deterministic design optimization and reliability analysis; the design optimization and reliability analysis are completed alternately and converge to the optimal solution. Currently, the decoupling approach has been the most effective type of method for addressing RBDO efficiency issue and has been the main research direction in RBDO. Wu et al. [13] used safety-factor-based deterministic constraints rather probabilistic constraints to avoid performing an inner-layer reliability analysis; however, this method can only consider the uncertainty in design parameters but cannot treat

random parameters. Du and Chen [14] proposed a sequential optimization and reliability assessment (SORA) algorithm based on the approximate equivalent feasible domain of the probabilistic constraints. This algorithm thus decouples the reliability analysis from the design optimization, significantly reducing the number of constraint reliability analysis and whereby improving the RBDO efficiency. Liang et al. [15] proposed a single-loop method (SLM) by using a similar searching strategy as the SORA algorithm. However, SLM utilizes an approximation method for reliability analysis to avoid multi-variable optimization in the conventional reliability computation and thus further improve the efficiency. Cheng et al. [16] divided the RBDO problem into a series of sub-problems by using linear approximation on the objective function and constraints, in which the reliability evaluation of constraints and sensitivity analysis could be conducted very efficiently. Shan and Wang [17] proposed a decoupling method that replaced probabilistic constraints with an approximate reliability design space and thus converted the RBDO problem into a deterministic optimization problem. However, it seems difficult for this method to treat problems that the probabilistic constraints are complex implicit functions. Agarwal et al. [18] employed homotopy analysis technique and Karush-Kuhn-Tucker condition to transform the original RBDO problem into a series of less difficult optimizations. Huang et al. [19], based on the SORA, obtained the most probable point (MPP) using an approximation strategy and thereby further improved the RBDO efficiency. Chen et al. [20] modified the solution framework of SORA by proposing a new shifting vector computation method when applying equivalent constraints, which reduced the number of iterations to a certain extent. Generally, the decoupling method could improve the RBDO computational efficiency significantly and greatly facilitate the application of RBDO in practical structural analysis and product design. However, objectively, the decoupling method currently still has some shortcomings. First, in terms of computational efficiency, although methods such as SORA have successfully separated reliability analysis from design optimization and thus eliminated two-layer nested optimization, the entire iterative solving process still needs to perform reliability analysis many times. Furthermore, every reliability analysis is a multi-variable optimization process, which makes these decoupling methods difficult to satisfy the design requirements of many more complex structures. The second shortcoming is related to the convergence of the computational processes. To reduce the computational cost incurred by the reliability analysis in the iterative process, some approximate reliability analysis strategies were then introduced in several current RBDO decoupling methods, such as SLM [15] and sequential approximate programming approach [16]. These strategies make the RBDO solution much more efficient. However, the introduction of these approximate reliability analysis strategies may decrease the convergence of the decoupling methods, thereby leading to difficulty in converging to a stable solution especially when treating problems with more variables and

relatively high degrees of non-linearity. Therefore, developing a decoupling method for RBDO that is efficient and also exhibits stable convergence is of great importance. Such a method will effectively improve the ability of RBDO to solve many more complex engineering problems and hence greatly increase the practical use of RBDO.

This paper proposes a new RBDO method based on an incremental shifting vector (ISV) strategy; it uses currently available decoupling methods as its foundation. This method exhibits a good comprehensive performance in terms of efficiency and convergence and hence provides an effective computation tool for reliability design of many complex structures and products. The remainder of this paper is structured as follows: the second section reviews the general concepts and decoupling strategies of RBDO, the third section proposes the ISV method, the fourth and fifth sections present the analyses of numerical examples and practical applications, respectively, and the sixth section discusses the conclusions.

2 Fundamental concepts and decoupling approach of RBDO

A RBDO problem can generally be expressed as follows [14]:

$$\begin{aligned} &\min_{\mathbf{d},\boldsymbol{\mu}_\mathbf{X}} f\left(\mathbf{d},\boldsymbol{\mu}_\mathbf{X},\boldsymbol{\mu}_\mathbf{P}\right) \\ &\text{s.t. } \operatorname{Prob}\left(g_j\left(\mathbf{d},\mathbf{X},\mathbf{P}\right)\ge 0\right)\ge R_j^{\mathrm{t}}, \quad j=1,2,...,n_g \\ &\qquad \mathbf{d}^{\mathrm{L}}\le\mathbf{d}\le\mathbf{d}^{\mathrm{U}}, \boldsymbol{\mu}_\mathbf{X}^{\mathrm{L}}\le\boldsymbol{\mu}_\mathbf{X}\le\boldsymbol{\mu}_\mathbf{X}^{\mathrm{U}} \end{aligned} \tag{1}$$

where f and g_j represent the objective function and j-th constraint, respectively; n_g represents the number of constraints; $\mathbf{d}$ represents the n_d-dimensional deterministic design vector; $\mathbf{X}$ represents the n_X-dimensional random design vector; $\mathbf{P}$ represents the n_p-dimensional random parameter vector; $\boldsymbol{\mu}_\mathbf{X}$ and $\boldsymbol{\mu}_\mathbf{P}$ represent the mean vectors of $\mathbf{X}$ and $\mathbf{P}$, respectively; and L and U represent the upper and lower boundaries, respectively; Prob represents the probability of constraint satisfaction, which is also called the reliability; and R_j^{t} represents the desired probability of the j-th constraint. In practical engineering applications, f and g_j are usually non-linear implicit functions; the former is related to $\mathbf{d}$, $\boldsymbol{\mu}_\mathbf{X}$, and $\boldsymbol{\mu}_\mathbf{P}$, and the latter is related to $\mathbf{d}$, $\mathbf{X}$, and $\mathbf{P}$.

Assume that $\mathbf{X}$ and $\mathbf{P}$ are mutually independent. Then, under any $\mathbf{d}$ and $\boldsymbol{\mu}_\mathbf{X}$, the reliability of the j-th constraint can be written in the following integral form:

$$\begin{aligned} &\operatorname{Prob}\left(g_j\left(\mathbf{Z}\right)\ge 0\right)=\int_{g_j\ge 0} h_\mathbf{Z}\left(\mathbf{Z}\right)d\mathbf{Z} \\ &\mathbf{Z}=\left[\mathbf{X},\mathbf{P}\right] \end{aligned} \tag{2}$$

Prof. G.I.N. Rozvany, phone: +36 (26) 362 592, e-mail: smo.rozvany@axelero.hu

where $\mathbf{Z}$ represents an n_Z-dimensional random vector with $\boldsymbol{\mu}_\mathbf{Z}$ as the mean vector, where $n_Z = n_X + n_P$, and $h_\mathbf{Z}(\mathbf{Z})$ represents the joint probability density function (PDF) of $\mathbf{Z}$.

2.1 Constraint reliability analysis

Currently, the first-order reliability method (FORM) is the most widely used method for treating the constraint reliability. Its basic idea is to map the constraint function from the original space (*Z* space) to the standard normal space (*U* space), construct linear approximation of the constraint function at the most probable point (MPP) and whereby compute the approximate reliability. The mapping of the random variables from *Z* space to *U* space can be expressed as follows [28, 29]:

$$\begin{aligned} &\Phi(U_i) = F_{Z_i}(Z_i), \qquad i = 1,2,...,n_Z \\ &U_i = \Phi^{-1}\left(F_{Z_i}(Z_i)\right),\ Z_i = F_{Z_i}^{-1}\left(\Phi(U_i)\right) \end{aligned} \tag{3}$$

where F_{Z_i} and $F_{Z_i}^{-1}$ are the cumulative distribution function (CDF) and its inverse function of Z_i, respectively; Φ and Φ^{-1} represent the standard normal CDF and its inverse function, respectively; and **U** is **Z** vector in the standard normal space. Then, the probabilistic constraint in Eq. (1) can be rewritten as follows:

$$\begin{aligned} &\text{Prob}\left(g_j(\mathbf{d},\mathbf{X},\mathbf{P}) \ge 0\right) = \int_{G_j \ge 0} h_\mathbf{U}(\mathbf{U}) d\mathbf{U} > R_j^t \\ &R_j^t = \Phi\left(-\beta_j^t\right), \qquad j = 1,2,...,n_g \end{aligned} \tag{4}$$

where G denotes the constraint function g in *U* space, $h_\mathbf{U}$ is the joint PDF of the standard normal vector $\mathbf{U}$, and β_j^t is the desired reliability index of the *j*-th constraint.

There are two kinds of commonly used FORMs to solve Eq. (4), the reliability index approach (RIA) [28-32] and the performance measurement approach (PMA) [33-37]. In RIA, the reliability index β represents the minimum distance between the limit-state surface and the origin in *U* space and can be expressed as follows:

$$\begin{aligned} &\beta = \min_\mathbf{U} \|\mathbf{U}\| \\ &\text{s.t. } G(\mathbf{U}) = 0 \end{aligned} \tag{5}$$

Its optimum solution $\mathbf{U}_{\text{MPP}}$ (which is the MPP) and reliability index β can be obtained through some well established methods such as the Hasofer-Lind and Rackwitz-Fiessler (HL-RF) iterations [28, 29]. If $\beta \ge \beta^t$, then the constraint can be considered to satisfy the reliability requirement. PMA, which is also called the inverse reliability analysis, generally can exhibit better performance than the RIA in RBDO problems because it uses a fixed search region [33]. In PMA, the location of the MPP can be determined through a following optimization problem:

$$\begin{aligned} &\min_{\mathbf{U}} G(\mathbf{U}) \\ &\text{s.t.} \left\|\mathbf{U}\right\| = \beta^{\mathrm{t}} \end{aligned} \tag{6}$$

The optimal solution $\mathbf{U}_{\mathrm{MPP}}$ and corresponding performance function value $G\left(\mathbf{U}_{\mathrm{MPP}}\right)$ can be obtained through some high-efficiency methods such as the advanced mean value method [34]. When $G\left(\mathbf{U}_{\mathrm{MPP}}\right) \geq 0$, the constraint can be considered to satisfy the reliability requirement.

2.2 Decoupling approach

Through the above analysis, it can be found that the solution of RBDO involves a two-layer nested optimization, which generally suffers from extremely low computational efficiency in practical applications. The decoupling method seems the most effective RBDO solution method that has been presented to date. Its basic idea is to convert the nested optimization into a sequential iteration process composed of a deterministic design optimization and the reliability analysis. The design optimization and reliability analysis are performed alternately; therefore, the computational cost is greatly reduced. Currently, SORA [14] and SLM [15] seem the two most important decoupling methods for RBDO, which have been successfully applied to many practical engineering problems.

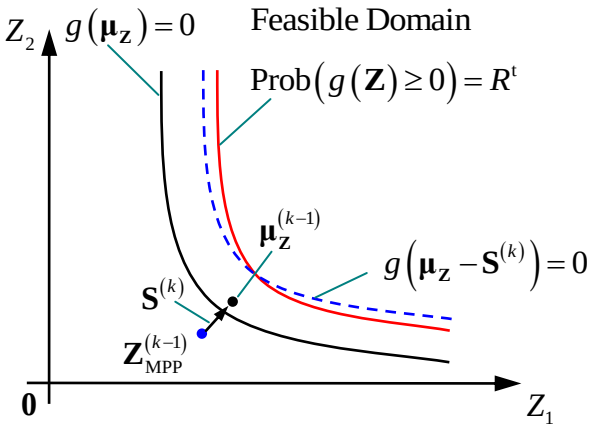

Fig. 1 Shifting vector of the probability constraint in SORA

In SORA, the key is to determine a deterministic constraint approximation that is equivalent to the probabilistic constraint, which requires construction of a shifting vector. For description convenience, assume that **d** does not exist and there are only **X** and **P**. The vector **Z** composed of **X** and **P** includes two normally distributed random components, and the equivalent process of a certain constrain in the *k*-th iteration is shown in Fig. 1. The curve $g\left(\boldsymbol{\mu}_{\mathbf{Z}}\right)=0$ represents the original boundary of the deterministic constraint. After considering the uncertainty, the feasible domain of the design variables is decreased, and the probabilistic constraint boundary, $\mathrm{Prob}\left(g\left(\mathbf{Z}\right)\geq 0\right)=R^{\mathrm{t}}$, must be inside the feasible domain of the deterministic constraint. In SORA, the approximate equivalent boundary of the actual probabilistic constraint boundary is obtained by moving the original boundary $g\left(\boldsymbol{\mu}_{\mathbf{Z}}\right)=0$ toward the feasible domain by a vector $\mathbf{S}$, which is denoted as $g\left(\boldsymbol{\mu}_{\mathbf{Z}}-\mathbf{S}^{(k)}\right)=0$. Then, in the *k*-th iteration, the converted deterministic design optimization can be created [14]:

Prof. G.I.N. Rozvany, phone: +36 (26) 362 592, e-mail: smo.rozvany@axelero.hu

$$\begin{aligned} &\min_{\mathbf{d},\boldsymbol{\mu}_\mathbf{X}} \ f\left(\mathbf{d},\boldsymbol{\mu}_\mathbf{X},\boldsymbol{\mu}_\mathbf{P}\right) \\ &\text{s.t. } \ g_j\left(\mathbf{d},\boldsymbol{\mu}_\mathbf{Z}-\mathbf{S}_j^{(k)}\right)\geq 0, \ \ j=1,2,...,n \\ &\qquad \boldsymbol{\mu}_\mathbf{Z}=\left[\boldsymbol{\mu}_\mathbf{X},\boldsymbol{\mu}_\mathbf{P}\right], \mathbf{d}^\mathrm{L}\leq\mathbf{d}\leq\mathbf{d}^\mathrm{U}, \boldsymbol{\mu}_\mathbf{X}^\mathrm{L}\leq\boldsymbol{\mu}_\mathbf{X}\leq\boldsymbol{\mu}_\mathbf{X}^\mathrm{U} \end{aligned} \tag{7}$$

The computation of the shifting vector **S** is the key of the method. **S** determines the difference between the probabilistic constraint boundary and the equivalent constraint boundary, and the smaller the difference, the faster the iterations can approach the optimal solution and the fewer number of iterations are required. However, the computation of **S** itself directly impacts the efficiency of RBDO.

In SORA, the shifting vector **S** depends on the MPP information in the previous iteration, $\mathbf{Z}^{(k\text{-}1)}$. It should be noted that MPP is different for different constraints; therefore, the shifting vectors of different constraints are generally not the same. For a specific constraint, the shifting vector can be written as:

$$\mathbf{S}^{(k)}=\boldsymbol{\mu}_\mathbf{Z}^{(k-1)}-\mathbf{Z}_\mathrm{MPP}^{(k\text{-}1)} \tag{8}$$

In the above equation, $\mathbf{Z}_\mathrm{MPP}^{(k\text{-}1)}$ can be obtained by solving the following PMA optimization:

$$\begin{aligned} &\min_{\mathbf{U}} G\left(\mathbf{d}^{(k-1)},\mathbf{U}\right) \\ &\text{s.t. } \ \left\|\mathbf{U}\right\|=\beta^\mathrm{t} \end{aligned} \tag{9}$$

The optimal solution of the above problem is $\mathbf{U}_\mathrm{MPP}^{(k\text{-}1)}$, and its value in the original space is $\mathbf{Z}_\mathrm{MPP}^{(k\text{-}1)}$. The design optimization in Eq. (7) and reliability analysis in Eq. (9) are performed alternately until convergence is achieved.

SLM [14] uses a solution framework similar as SORA. The *k*-th iteration step also contains a deterministic design optimization as indicated in Eq. (7), and for a certain constraint the computation of the shifting vector $\mathbf{S}^{(k)}$ also depends on the corresponding MPP of the previous step as in Eq. (8). The difference is that SLM computes an imprecise MPP using an approximate reliability analysis technique to construct the shifting vector in each iteration step. Thus the inner layer optimization for reliability analysis is eliminated, and whereby the whole optimization efficiency can be greatly promoted.

3 Formulation of the ISV method

It can be observed from the above analysis that when the reliability analysis is decoupled from the design optimization in SORA, the efficiency is improved greatly compared with the earlier two-layer nested optimization. However, it can also be observed that the whole optimization process still needs a number of reliability analyses, especially for problems with more constraints. Furthermore, every reliability analysis needs to solve a time-consuming optimization problem; therefore, the computational cost seems still a challenge for SORA when dealing with some more complex engineering problems. The special feature of SLM is that an approximation technique is used when computing the MPP; therefore, it avoids the optimization solution for reliability analysis, and the computational efficiency is improved further relative to SORA. However, the introduction of approximate

Prof. G.I.N. Rozvany, phone: +36 (26) 362 592, e-mail: smo.rozvany@axelero.hu

reliability analysis can lead to divergence in the iteration process and thus decrease the stability and convergence of the decoupling process greatly; this will be demonstrated in the examples presented below. In the following, this paper will propose a new decoupling method for RBDO, namely the incremental shifting vector approach (ISV). The proposed method exhibits a better overall performance in terms of efficiency and convergence and expects to provide an effective computational tool for reliability design of many complex structures and products in the future. The ISV method uses a similar solution framework as SORA and SLM, i.e., converting a multilayer nested optimization into the sequential design optimization and reliability analysis steps. Compared with the currently available methods, the innovations of ISV are that it uses an incremental shifting strategy to ensure stable convergence in the iteration process and that it also provides a new computational method for determining the shifting vector in the incremental iteration process to ensure high efficiency of RBDO.

3.1 Incremental shifting strategy

In the currently available decoupling strategies such as SORA and SLM, as indicated by Eq. (7), the constraint boundary needs to be determined by computing the shifting vector $\mathbf{S}_j^{(k)}$ based on the original boundary $g_j\left(\mathbf{d},\boldsymbol{\mu}_\mathbf{Z}\right)=0$ in any iteration step *k*; this makes the deterministic constraint $g_j\left(\mathbf{d},\boldsymbol{\mu}_\mathbf{Z}-\mathbf{S}_j^{(k)}\right)\geq 0$ equivalent to the probabilistic constraint $\mathrm{Prob}\left(g_j\left(\mathbf{d},\mathbf{X},\mathbf{P}\right)\geq 0\right)\geq R_j^{\mathrm{t}}$ in Eq. (1). Consequently, the shifting vectors need to be recomputed in each iteration. For some complex RBDO problems, such as functions with strong non-linearity or when the number of constraints or variables is relatively large, the difference between the shifting vectors of two adjacent iteration steps can be large, which may lead to numerical oscillation and whereby impact the convergence of the iteration process. Especially for methods such as SLM that use an approximate reliability analysis, the difficulty for the entire decoupling method to converge is exacerbated if the shifting vector must be recomputed in every iteration. To address the above issue, only a shifting vector increment $\Delta\mathbf{S}^{(k)}$ is computed in the *k*-th iteration step of the ISV method. This shifting vector increment is then combined with the shifting vector $\mathbf{S}^{(k-1)}$ in the previous step to form the current shifting vector $\mathbf{S}^{(k)}$:

$$\mathbf{S}^{(k)}=\mathbf{S}^{(k-1)}+\Delta\mathbf{S}^{(k)} \tag{10}$$

Using $\mathbf{S}^{(k)}$, the deterministic design optimization problem, as given by Eq. (7), can be created and solved. Therefore, in ISV the shifting vector in each iteration step is only an adjustment to the shifting vector in the previous step, and the shift of the constraint boundary is incremental.

Prof. G.I.N. Rozvany, phone: +36 (26) 362 592, e-mail: smo.rozvany@axelero.hu

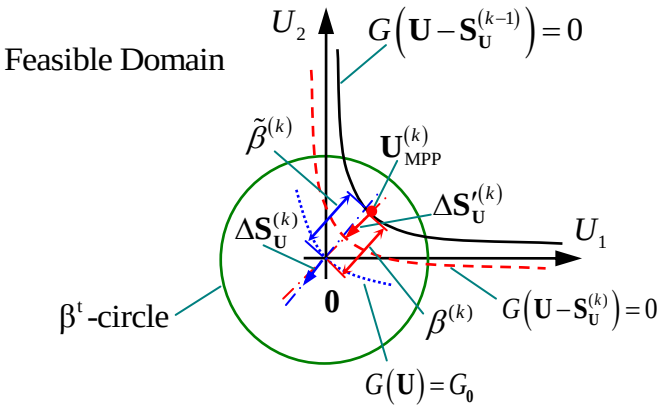

Fig. 2 Shifting vector increment in ISV method

We use Fig. 2 to illustrate the computational process for determining the shifting vector increment of a constraint in the *k*-th iteration. For convenience of description, we assume there are 2 random variables in the constraint, and the entire analysis process takes place in *U* space. The curve $G\left(\mathbf{U}-\mathbf{S}_{\mathbf{U}}^{(k-1)}\right)=0$ represents the equivalent constraint boundary of the previous iteration step, and its left side is the feasible domain, within which the current design falls. It is noted that the optimum $\boldsymbol{\mu}_{\mathbf{Z}}^{(k)}$ is updated; hence the constraint function G in *U* space is related to the iteration *k*. Considering the uncertainty, the random space of the design is centered at the origin, and the target reliability index is a circle with the radius β^{t}, which is referred to as the β^{t}-circle. Assuming that the constraint boundary $G\left(\mathbf{U}-\mathbf{S}_{\mathbf{U}}^{(k-1)}\right)=0$ passes through the β^{t}-circle, then the actual reliability index β is less than the target reliability index β^{t}; in this case, the reliability requirement is not satisfied, and the difference is $\Delta\beta=\beta^{\mathrm{t}}-\beta$. To improve the design reliability, the constraint boundary should be adjusted toward the feasible domain in the current iteration step. Specifically, the equivalent constraint boundary needs to be shifted from where it was in the previous iteration by $\Delta\beta$ in the MPP gradient direction. It is just the shifting vector increment that needs to compute in our ISV approach, and it can be expressed as:

$$\Delta\mathbf{S}_{\mathbf{U}}^{(k)}=\left(\beta^{\mathrm{t}}-\beta^{(k)}\right)\left(-\frac{\nabla G\left(\mathbf{U}_{\mathrm{MPP}}^{(k)}\right)}{\left\|\nabla G\left(\mathbf{U}_{\mathrm{MPP}}^{(k)}\right)\right\|}\right) \tag{11}$$

If we solve the above equation directly, then RIA must be used to obtain $\beta^{(k)}$ and $\mathbf{U}_{\mathrm{MPP}}^{(k)}$ to determine the shifting vector increment. However, the form of RIA is a multi-variant optimization problem as given by Eq. (5), which will lead to significant computational cost in practical engineering problems. In the following, an efficient method will be presented to solve Eq. (11).

As shown in Fig. 2, for a constraint that does not yet satisfy the reliability requirement, the $\mathbf{U}_{\mathrm{MPP}}$ is relatively

Prof. G.I.N. Rozvany, phone: +36 (26) 362 592, e-mail: smo.rozvany@axelero.hu

close to the mean value point $\mathbf{U_0}$ (the origin of *U* space). The contour of the constraint function $G(\mathbf{U}) = G_0$ (G_0 is the value of the constraint function at the origin of the *U* space) will have a curve shape that is very similar to the constraint boundary $G(\mathbf{U}) = 0$ under usual circumstances. Therefore, to solve Eq. (11), we can use the gradients at the origin $\mathbf{U_0} = \mathbf{0}$ to approximate the gradients at $\mathbf{U}_{\text{MPP}}$ and whereby compute an approximate reliability index $\tilde{\beta}^{(k)}$. The solution process can be expressed as:

$$G\left(-\tilde{\beta}^{(k)}\frac{\nabla G(\mathbf{U_0})}{\left\|\nabla G(\mathbf{U_0})\right\|}\right) = 0 \tag{12}$$

The above equation is a nonlinear equation that contains only one unknown variable $\tilde{\beta}^{(k)}$, which can be solved with high efficiency using the Newton iterative method [38]:

$$\left(\tilde{\beta}^{(k)}\right)_{j+1} = \left(\tilde{\beta}^{(k)}\right)_j + \frac{\left\|\nabla G(\mathbf{U_0})\right\|}{\nabla G(\mathbf{U_0})}\frac{G\left(-\left(\tilde{\beta}^{(k)}\right)_j\frac{\nabla G(\mathbf{U_0})}{\left\|\nabla G(\mathbf{U_0})\right\|}\right)}{G'\left(-\left(\tilde{\beta}^{(k)}\right)_j\frac{\nabla G(\mathbf{U_0})}{\left\|\nabla G(\mathbf{U_0})\right\|}\right)} \tag{13}$$

where *j* denotes the iteration step. Under normal circumstances, Newton iteration only requires a few steps and a small number of function computations to converge. Based on the above analysis, Eq. (11) can be rewritten as:

$$\Delta\mathbf{S}_{\mathbf{U}}^{(k)} = \left(\beta^t - \tilde{\beta}^{(k)}\right)\left(-\frac{\nabla G(\mathbf{U_0})}{\left\|\nabla G(\mathbf{U_0})\right\|}\right) \tag{14}$$

Mapping $\Delta\mathbf{S}_{\mathbf{U}}^{(k)}$ back to the original space through Eq. (3), the needed shifting vector increment $\Delta\mathbf{S}^{(k)}$ can be obtained.

3.2 Constraint reliability assessment

In practical RBDO problems, there can be many probabilistic constraints, some of which have relatively good reliability and always satisfy the reliability requirements in the iteration process. To further increase the efficiency, if a certain constraint in the current design satisfies the reliability requirement, then there is no need to shift the vector that corresponds to this constraint in the next iteration, i.e., we can set $\Delta\mathbf{S}^{(k)} = \mathbf{0}$; thus, a constraint reliability satisfaction assessment is needed. In PMA analysis, the reliability satisfaction of a certain constraint can be assessed through the following equation:

Prof. G.I.N. Rozvany, phone: +36 (26) 362 592, e-mail: smo.rozvany@axelero.hu

$$G\left(\mathbf{U}_{\mathrm{MPP}}^{(k-1)}\right)=G\left(-\beta^{\mathrm{t}}\frac{\nabla G\left(\mathbf{U}_{\mathrm{MPP}}^{(k-1)}\right)}{\left\|\nabla G\left(\mathbf{U}_{\mathrm{MPP}}^{(k-1)}\right)\right\|}\right)\geq 0 \tag{15}$$

It needs to solve an optimization problem as Eq. (6) to obtain the MPP [34]. As mentioned above, for the constraints that we are primarily concerned (constraints those do not satisfy the reliability requirements), the gradients at $\mathbf{U}_{\mathbf{0}}$ and at $\mathbf{U}_{\mathrm{MPP}}$ are generally very similar. Therefore, the proposed method uses the gradients at $\mathbf{U}_{\mathbf{0}}$ to approximate those at $\mathbf{U}_{\mathrm{MPP}}$ to reduce the computational cost; then, the reliability assessment in Eq. (15) can be changed to:

$$G\left(-\beta^{\mathrm{t}}\frac{\nabla G\left(\mathbf{U}_{\mathbf{0}}\right)}{\left\|\nabla G\left(\mathbf{U}_{\mathbf{0}}\right)\right\|}\right)\geq 0 \tag{16}$$

In doing so, the inverse MPP search required in Eq. (15) can be avoided. In each iteration, the reliability satisfaction of all probabilistic constraints is judged through Eq. (16), and the shifting vectors are only updated for the constraints that do not satisfy the reliability requirements.

Prof. G.I.N. Rozvany, phone: +36 (26) 362 592, e-mail: smo.rozvany@axelero.hu

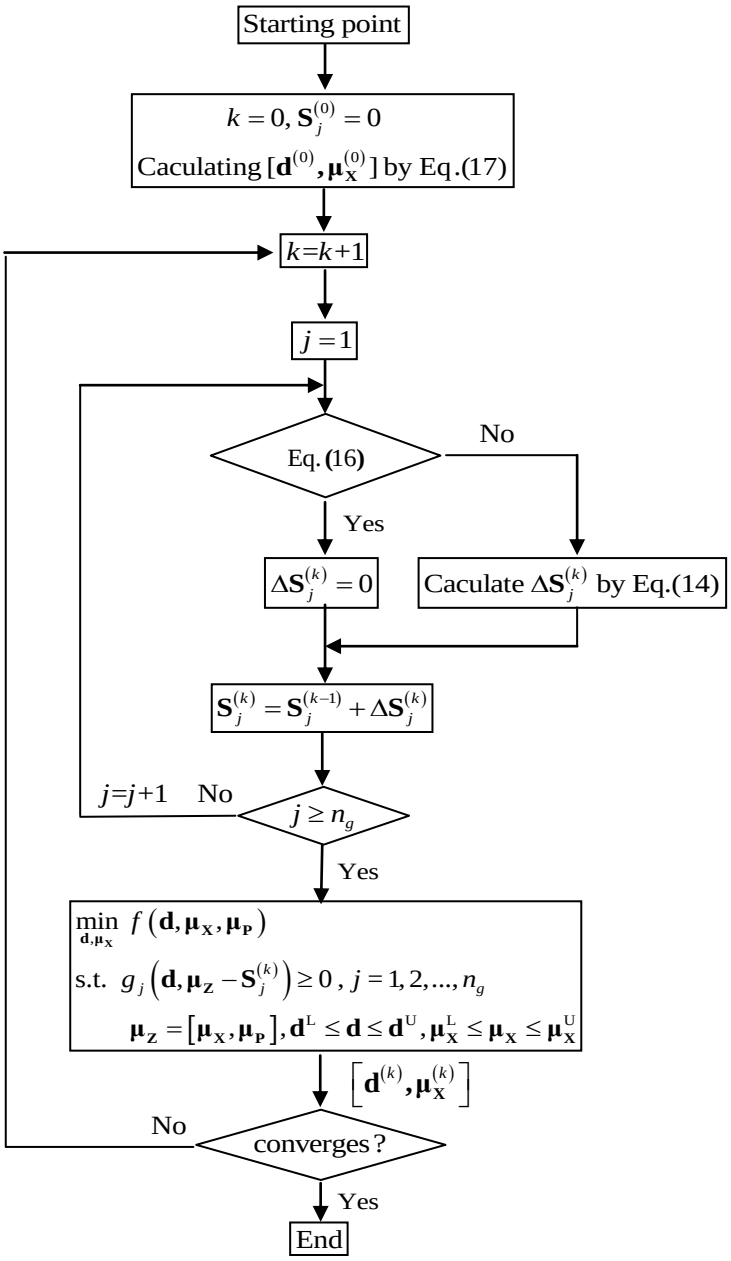

Fig. 3 Flowchart of the ISV method

3.3 Flowchart of the algorithm

The flowchart of our ISV method is shown in Fig. 3. The entire solving process is completed with a series of iteration steps. In every step, the constraint reliability satisfaction is assessed first. For those constraints that satisfy the reliability requirements, set the shifting vector increment to $\Delta\mathbf{S}^{(k)}=\mathbf{0}$; for those that do not satisfy the reliability requirements, the shifting vector increment analysis is conducted. The shifting vector $\mathbf{S}^{(k)}$ is obtained based on $\Delta\mathbf{S}^{(k)}$, and the design optimization problem in Eq. (7) is constructed and solved. The shifting vector computation and design optimization steps are conducted alternately until convergence is achieved. In theory, any

Prof. G.I.N. Rozvany, phone: +36 (26) 362 592, e-mail: smo.rozvany@axelero.hu

point could be used as the initial point of the ISV method, but to increase the convergence speed, the following deterministic optimization solution can be used as the initial point:

$$\begin{aligned} &\min_{\mathbf{d},\boldsymbol{\mu}_\mathbf{X}} f\left(\mathbf{d},\boldsymbol{\mu}_\mathbf{X},\boldsymbol{\mu}_\mathbf{P}\right) \\ &\text{s.t. } g_j\left(\mathbf{d},\boldsymbol{\mu}_\mathbf{Z}\right)\ge 0,\ j=1,2,...,n_g \\ &\quad \boldsymbol{\mu}_\mathbf{Z}=\left[\boldsymbol{\mu}_\mathbf{X},\boldsymbol{\mu}_\mathbf{P}\right],\mathbf{d}^\mathrm{L}\le\mathbf{d}\le\mathbf{d}^\mathrm{U},\boldsymbol{\mu}_\mathbf{X}^\mathrm{L}\le\boldsymbol{\mu}_\mathbf{X}\le\boldsymbol{\mu}_\mathbf{X}^\mathrm{U} \end{aligned} \tag{17}$$

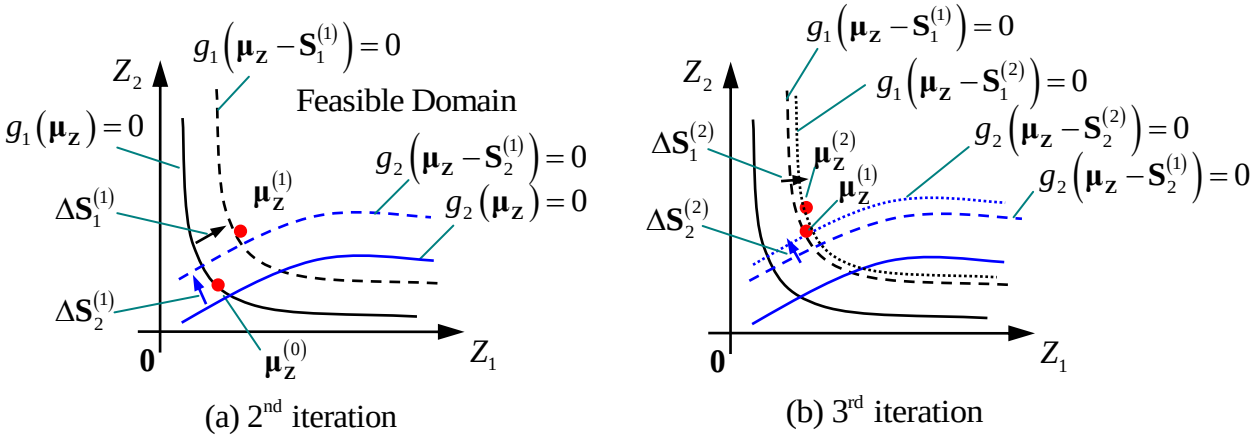

Fig. 4 Schematic diagram of the ISV's iterative process for a RBDO problem

As shown in Fig. 4, for the ease of understanding, a RBDO problem with 2 constraints is used to illustrate the iteration process of ISV. It is assumed that the vector **Z** contains 2 normal random variables, *X* and *P*. First, set the shifting vectors to $\mathbf{S}_1^{(0)}=0$ and $\mathbf{S}_2^{(0)}=0$ and solve Eq. (17) for the initial solution $\boldsymbol{\mu}_\mathbf{Z}^{(0)}$. We assume that this solution is located on the boundary of constraint 1, $g_1\left(\boldsymbol{\mu}_\mathbf{Z}\right)=0$, and close to the boundary of constraint 2, $g_2\left(\boldsymbol{\mu}_\mathbf{Z}\right)=0$; then, iteration 2 is entered. The reliability of every constraint is assessed with Eq. (16). Let us assume that neither of the two constraints satisfies the reliability requirement; then, Eq. (14) is used to compute the shifting vector increments $\Delta\mathbf{S}_1^{(1)}$ and $\Delta\mathbf{S}_2^{(1)}$ of the 2 constraint boundaries. Because the shifting vectors of the 2 constraints in the initial iteration are $\mathbf{S}_1^{(0)}=0$ and $\mathbf{S}_2^{(0)}=0$, the shifting vectors in the second iteration are $\mathbf{S}_1^{(1)}=\Delta\mathbf{S}_1^{(1)}$ and $\mathbf{S}_2^{(1)}=\Delta\mathbf{S}_2^{(1)}$, respectively. As shown in Fig. 4(a), the two constraint boundaries moved from their original places, $g_1\left(\boldsymbol{\mu}_\mathbf{Z}\right)=0$ and $g_2\left(\boldsymbol{\mu}_\mathbf{Z}\right)=0$, toward the feasible domain, and the equivalent constraint boundaries, $g_1\left(\boldsymbol{\mu}_\mathbf{Z}-\mathbf{S}_1^{(1)}\right)=0$ and $g_2\left(\boldsymbol{\mu}_\mathbf{Z}-\mathbf{S}_2^{(1)}\right)=0$, are obtained. The optimal solution $\boldsymbol{\mu}_\mathbf{Z}^{(1)}$ in the second iteration can be obtained by solving the design optimization problem like Eq. (7). Under the influence of the equivalent constraints, $\boldsymbol{\mu}_\mathbf{Z}^{(1)}$ moved toward the feasible domain relative to $\boldsymbol{\mu}_\mathbf{Z}^{(0)}$ and created a certain distance from the initial boundaries of the two constraints, which is reflected in the increase of the reliability of $\boldsymbol{\mu}_\mathbf{Z}^{(1)}$.

Prof. G.I.N. Rozvany, phone: +36 (26) 362 592, e-mail: smo.rozvany@axelero.hu

Then, the third iteration is entered. As before, Eq. (16) is used to assess the reliability of every constraint. Assume that the 2 constraints still do not satisfy the requirements. Then, Eq. (14) is used to compute the shifting vector increments $\Delta\mathbf{S}_1^{(2)}$ and $\Delta\mathbf{S}_2^{(2)}$, and the shifting vectors of the 2 constraints, $\mathbf{S}_1^{(2)} = \mathbf{S}_1^{(1)} + \Delta\mathbf{S}_1^{(2)}$ and $\mathbf{S}_2^{(2)} = \mathbf{S}_2^{(1)} + \Delta\mathbf{S}_2^{(2)}$, are computed. As shown in Fig. 4(b), the two constraint boundaries are incrementally adjusted based on their individual locations in the previous iteration, i.e., they are moved toward the feasible domain by a corresponding increment. Thus, the optimal solution $\boldsymbol{\mu}_{\mathbf{Z}}^{(2)}$ in the third iteration can be obtained by solving the design optimization problem specified by Eq. (7) again. The above iteration process will be repeated until convergence is achieved.

It can be observed based on the above analysis that in ISV approach the shifting vectors in each iteration step preserved their information from the previous step; thus, the shifting vectors can be considered as an adjustment to the ones of the previous iteration. Therefore, the equivalent constraint boundary is also an incremental adjustment from that of the previous iteration, and the movement of the constraint boundary is incremental. Such an incremental adjustment ensures that the locations of the constraint boundaries will not change drastically between two adjacent iterations; therefore, the method avoids numerical oscillation in the iteration process to a great extent. Simultaneously, the design reliability is increased stably, and convergence of the iterative process can be well guaranteed. Furthermore, the multi-variant optimization of the RIA reliability analysis is replaced by a determination of a solution to a non-linear equation (single-variable problem) in the computation of the shifting vector increment; thus, the computational cost is greatly reduced. Additionally, because of the adoption of an incremental shifting strategy, generally the small error introduced by the approximation in the shifting vector analysis does not take large influence to the convergence of the entire solution process, which gives ISV approach a good overall performance in terms of both efficiency and convergence. This point will be further demonstrated in the numerical examples that follow.

4 Numerical examples and discussion

In this section, six commonly used numerical examples in RBDO field are analyzed. As indicated in Table 1, these six examples have different complexities. There are five different situations that will be analyzed for each example. In situations 1 – 4, all random parameter distributions in a given situation are of the same type; in situations 1, 2, 3, and 4, respectively, normal, lognormal, uniform and Gumbel probability distributions, which are four typical probability distributions, are used. The fifth situation represents a general mixed situation, i.e., the random parameters are mixed with the above four distribution types. There are $6\times5=30$ situations in total. For every situation, SORA, SLM, and the ISV method proposed in this paper are used for optimization. The initial points used in all three methods are determined by using the deterministic optimization, and the convergence standards are set the same. The inverse MPP search in the SORA method and the design optimizations in the iterative processes of all three methods are solved using sequential quadratic programming (SQP) [39]. For every example, the optimum solution, number of iterations N_I, number of constraint function computations N_F, and actual reliability index β of the probabilistic constraints under the optimum solution from the three methods will be compared.

Prof. G.I.N. Rozvany, phone: +36 (26) 362 592, e-mail: smo.rozvany@axelero.hu

Table 1. Six numerical examples

Example	Random Design Variables	Random Parameters	Probabilistic Constrains	Reference
1	2	0	3	Liang et al. [15]
2	0	4	2	Liang et al. [15]
3	2	0	2	Chen et al. [20]
4	5	0	10	Chen et al. [20]
5	4	6	1	Cheng et al. [16]
6	4	7	5	Cho et al. [27]

4.1 Example 1

Consider the following RBDO problem [15]:

$$\begin{aligned}
&\min_{\boldsymbol{\mu}_{\mathbf{X}}} \; f\left(\boldsymbol{\mu}_{\mathbf{X}}\right)=\mu_{X_1}+\mu_{X_2} \\
&\text{s.t. } \operatorname{Prob}\left(g_j\left(\mathbf{X}\right)\geq 0\right)\geq \Phi\left(-\beta_j^{\mathrm{t}}\right),\ \beta_j^{\mathrm{t}}=3.0,\ j=1,2,3 \\
&\qquad g_1\left(\mathbf{X}\right)=\frac{X_1^2X_2}{20}-1 \\
&\qquad g_2\left(\mathbf{X}\right)=\frac{\left(X_1+X_2-5\right)^2}{30}+\frac{\left(X_1-X_2-12\right)^2}{120}-1 \\
&\qquad g_3\left(\mathbf{X}\right)=\frac{80}{\left(X_1^2+8X_2+5\right)}-1 \\
&\qquad 0\leq \mu_{X_i}\leq 10, \sigma_{X_i}=0.3, i=1,2
\end{aligned} \tag{18}$$

where μ_{X_i} and σ_{X_i} represent the mean and standard deviation of the random design variable X_i, respectively.

The computational results are presented in Table 2. It can be observed from the results that for the five different distribution situations SORA and ISV converged to very close results, but in the third situation, for which all random variables have uniform distributions, the SLM diverged. The reason is that in SLM the MPP of the current iteration will be approximately replaced by the MPP in the previous iteration to construct the shifting vector. However, in the first iteration in this example, neither of the two components of the MPP of the constraint g_1, $\mathbf{X}_{\mathrm{MPP}}^{(0)}=\left[2.599,1.587\right]$, lies within the uniform distribution region of the design in the second iteration, $\boldsymbol{\mu}_{\mathbf{X}}^{(1)}=\left[3.341,2.980\right]$ ($\mathbf{I}_{X_1}=\left[2.839,3.843\right]$ and $\mathbf{I}_{X_2}=\left[2.478,3.482\right]$), which renders obtaining an approximation of MPP in the current iteration impossible and leads to a failure to converge.

Prof. G.I.N. Rozvany, phone: +36 (26) 362 592, e-mail: smo.rozvany@axelero.hu

Table 2. Optimization results for numerical example 1

Distribution	Results	SORA	SLM	ISV
X_1, X_2: Normal	$\boldsymbol{\mu}_{\mathbf{x}}^*$	3.439, 3.287	3.440, 3.284	3.440, 3.281
	f^*	6.726	6.724	6.721
	N_I	3	4	4
	N_F	183	76	99
	$\boldsymbol{\beta}$	3.0, 3.0, 10.0	3.0, 3.0, 10.0	3.0, 3.0, 10.0
X_1, X_2: Lognormal	$\boldsymbol{\mu}_{\mathbf{x}}^*$	3.401, 3.186	3.401, 3.185	3.415, 3.197
	f^*	6.587	6.586	6.612
	N_I	3	6	3
	N_F	178	106	102
	$\boldsymbol{\beta}$	3.0, 3.0, 7.8	3.0, 3.0, 7.8	3.1, 3.0, 7.8
X_1, X_2: Uniform	$\boldsymbol{\mu}_{\mathbf{x}}^*$	3.343, 2.981	---	3.341, 2.980
	f^*	6.324	---	6.321
	N_I	2	---	2
	N_F	217	---	53
	$\boldsymbol{\beta}$	3.0, 2.9, 3.9	---	2.9, 3.0, 3.9
X_1, X_2: Gumbel	$\boldsymbol{\mu}_{\mathbf{x}}^*$	3.280, 3.010	3.288, 2.996	3.312,3.018
	f^*	6.290	6.284	6.330
	N_I	3	6	2
	N_F	183	118	51
	$\boldsymbol{\beta}$	3.0, 3.0, 5.34	2.9, 3.0, 5.3	3.2, 3.0, 5.3
X_1: Normal X_2:Lognormal	$\boldsymbol{\mu}_{\mathbf{x}}^*$	3.471, 3.208	3.472, 3.207	3.464, 3.222
	f^*	6.680	6.679	6.686
	N_I	3	6	3
	N_F	188	112	78
	$\boldsymbol{\beta}$	3.0, 3.0, 8.9	3.0, 3.0, 8.9	3.0, 3.0, 8.9

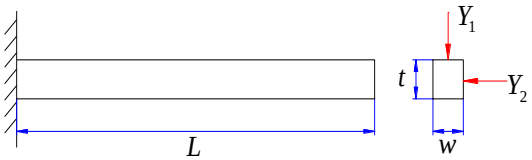

Fig. 5 A cantilever beam [15]

Prof. G.I.N. Rozvany, phone: +36 (26) 362 592, e-mail: smo.rozvany@axelero.hu

4.2 Example 2

As shown in Fig. 5, the example represents a cantilever bending problem under a load. The free end of the cantilever is under a vertical load of Y_1 and a horizontal load of Y_2, The width *w* and thickness *t* of the cross-section of the cantilever are deterministic design variables, and the design target is the weight of the cantilever. Two failure modes are considered: the first is that the stress at the fixed end should not be greater than the allowable yield stress *y*, and the second is that the displacement of the free end should not be greater than the allowable displacement $D_0 = 2.5\,\text{in}$. The length of the cantilever is $L = 100\,\text{in}$, *E* is the Young's Modulus, and the material density is constant. The RBDO problem can be created as follows [15]:

$$\begin{aligned}
&\min_{w,t}\ f(w,t) = wt \\
&\text{s.t. } \text{Prob}\left(g_j(w,t,Y_1,Y_2,y,E)\right) \ge 0 \ge \Phi\left(-\beta_j^{\text{t}}\right),\ \beta_j^{\text{t}} = 3.0,\ \ j = 1,2 \\
&\qquad g_1(w,t,Y_1,Y_2,y) = y - \left(\frac{600}{wt^2}Y_1 + \frac{600}{w^2 t}Y_2\right) \\
&\qquad g_2(w,t,Y_1,Y_2,E) = D_0 - \frac{4L^3}{Ewt}\sqrt{\left(\frac{Y_1}{t^2}\right)^2 + \left(\frac{Y_2}{w^2}\right)^2} \\
&\qquad w > 0\,\text{in},\ \ 0\ \text{in} < t < 5\,\text{in}
\end{aligned} \tag{19}$$

where the loads Y_1 and Y_2, the allowable yield stress *y*, and the Young's Modulus *E* are random parameters as shown in Table 3.

Table 3. Random variables and distributions in example 2

Variable	Symbol	Mean	Standard deviation
Vertical load	Y_1	1000 lb	100 lb
Horizontal load	Y_2	500 lb	50 lb
Allowable yield stress	*y*	40000 psi	4000 psi
Young's Modulus	*E*	29000000 psi	2900000 psi

4.3 Example 3

Consider the following RBDO problem [20]:

$$\begin{aligned}
&\min_{\boldsymbol{\mu}_{\mathbf{X}}}\ f(\boldsymbol{\mu}_{\mathbf{X}}) = \left(\mu_{X_1} - 3.7\right)^2 + \left(\mu_{X_2} - 4\right)^2 \\
&\text{s.t. } \text{Prob}\left(g_j(\mathbf{X}) \ge 0\right) \ge \Phi\left(-\beta_j^{\text{t}}\right),\ \ \beta_j^{\text{t}} = 2.0,\ j = 1,2 \\
&\qquad g_1(\mathbf{X}) = -X_1 \sin\left(4X_1\right) - 1.1X_2 \sin\left(2X_2\right) \\
&\qquad g_2(\mathbf{X}) = X_1 + X_2 - 3 \\
&\qquad 0.0 \le \mu_{X_1} \le 3.7\ \ 0.0 \le \mu_{X_2} \le 4.0 \\
&\qquad \sigma_{X_i} = 0.1,\ i = 1,2
\end{aligned} \tag{20}$$

Prof. G.I.N. Rozvany, phone: +36 (26) 362 592, e-mail: smo.rozvany@axelero.hu

There are two random design variables and two probabilistic constraints.

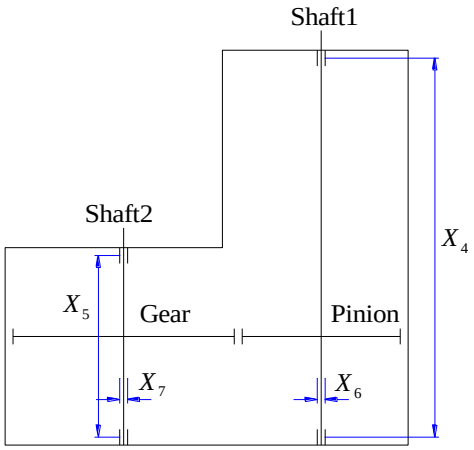

Fig. 6 A speed reducer of light plane [20]

Table 4. Random variables and distributions in example 4

Variable	Symbol	Mean	Standard deviation
Gear width	X_1	μ_{X1}	0.005 mm
Shaft1 length	X_2	μ_{X2}	0.005 mm
Shaft2 length	X_3	μ_{X3}	0.005 mm
Shaft1 diameter	X_4	μ_{X4}	0.005 mm
Shaft2 diameter	X_5	μ_{X5}	0.005 mm

4.4 Example 4

Figure 6 illustrates a speed reducer on a light plane. The speed reducer can realize high-efficiency speed matching between the engine and the propeller. The design target is to minimize the weight of the speed reducer. This problem contains 2 deterministic design variables, 5 random design variables as shown in Table 4 and 10 probabilistic constraints. The deterministic design variables include the pinion teeth number d_1 and gear module d_2. And the random design variables include the gear width X_1, the gear modulus X_2, the number of pinion teeth X_3, the lengths of shaft 1 and shaft 2 denoted as X_4 and X_5, the diameters of shaft 1 and shaft 2 denoted as X_6 and X_7, and all variables are mutually independent. The probabilistic constraints involve several mechanical properties of the speed reducer, such as bending stress, contact stress, longitudinal displacement, axial displacement, and geometrical dimension constraints. The RBDO model of the speed reducer can be created in the following form [20]:

Prof. G.I.N. Rozvany, phone: +36 (26) 362 592, e-mail: smo.rozvany@axelero.hu

$$\min_{\mathbf{d},\boldsymbol{\mu}_\mathbf{X}} f\left(\mathbf{d},\boldsymbol{\mu}_\mathbf{X}\right)=0.7854\mu_{X_1}d_2\left(3.3333d_1^2+14.9334d_1-43.0934\right)$$
$$-1.508d_1\left(\mu_{X_4}^2+\mu_{X_5}^2\right)+7.477\left(\mu_{X_4}^3+\mu_{X_5}^3\right)+0.7854\left(d_1\mu_{X_4}^2+\mu_{X_2}\mu_{X_5}^2\right)$$
$$\text{s.t. } \text{Prob}\left(g_j\left(\mathbf{d},\boldsymbol{\mu}_\mathbf{X}\right)\ge 0\right)\ge \Phi\left(-\beta_j^{\text{t}}\right),\ \beta_j^{\text{t}}=3.0,\ j=1,2,...,10$$
$$g_1\left(\mathbf{d},\mathbf{X}\right)=1-\frac{27}{d_1d_2^2X_1},\ g_2\left(\mathbf{d},\mathbf{X}\right)=1-\frac{397.5}{d_1^2d_2^2X_1},\ g_3\left(\mathbf{d},\mathbf{X}\right)=1-\frac{1.93X_2^3}{d_2d_1X_4^4},$$
$$g_4\left(\mathbf{d},\mathbf{X}\right)=1-\frac{1.93X_3^3}{d_2d_1X_5^4},\ g_5\left(\mathbf{d},\mathbf{X}\right)=1100-\frac{\sqrt{\left[745X_2/(d_2d_1)\right]^2+16.9\times10^6}}{0.1X_4^3}$$
$$g_6\left(\mathbf{d},\mathbf{X}\right)=850-\frac{\sqrt{\left[745X_3/(d_2d_1)\right]^2+157.5\times10^6}}{0.1X_5^3},\ g_7(\mathbf{d},\mathbf{X})=\frac{X_1}{d_2}-5,$$
$$g_8(\mathbf{d},\mathbf{X})=12-\frac{X_1}{d_2},\ g_9\left(\mathbf{X}\right)=1-\frac{1.5X_4+1.9}{X_2},\quad g_{10}\left(\mathbf{X}\right)=1-\frac{1.1X_5+1.9}{X_3},$$
$$17\le d_1\le 18,\ 0.7\text{mm}\le d_2\le 0.8\text{mm},\ 2.6\text{mm}\le\mu_{X_1}\le 3.6\text{mm},\ 7.3\text{mm}\le\mu_{X_2}\le 8.3\text{mm},$$
$$7.3\text{mm}\le\mu_{X_3}\le 8.3\text{mm},\ 2.9\text{mm}\le\mu_{X_4}\le 3.9\text{mm},\ 5.0\text{mm}\le\mu_{X_5}\le 5.5\text{mm} \tag{21}$$

4.5 Example 5

Consider the design problem of a steel column. The column length is a constant, and the cross-sectional dimensions *B*, *D* and *H* are three random design variables. The design target is to minimize the volume of the column, and there is only one failure mode. The RBDO problem can be expressed as [16]:

$$\min_{\mu_B,\mu_D,\mu_H} f(\mu_B,\mu_D,\mu_H)=\mu_B\mu_D+5\mu_H$$
$$\text{s.t. } \text{Prob}\left(g\left(B,D,H,F_S,P_1,P_2,P_3,F_0,E\right)\ge 0\right)\ge\Phi\left(-\beta^{\text{t}}\right),\ \beta^{\text{t}}=3.0$$
$$g=F_S-F\left(\frac{1}{A_S}+\frac{F_0}{U_s}\frac{\varepsilon_b}{\varepsilon_b-F}\right)$$
$$200\text{mm}\le\mu_B\le 400\text{mm},\ 10\text{mm}\le\mu_D\le 30\text{mm},$$
$$100\text{mm}\le\mu_H\le 500\text{mm}, \tag{22}$$
$$\text{where } A_s=2BD,\ U_s=BDH,\ \varepsilon_b=\frac{\pi^2EU_i}{L^2},$$
$$U_i=\frac{1}{2}BDH^2,\ F=P_1+P_2+P_3,\ L=7500\text{mm}$$

where the random design variables are flange breadth *B*, flange thickness *D* and height of profile *H*; the random parameters are yield stress F_S, dead weigh load P_1, variable load P_2, variable load P_3, initial deflection F_0 and Young's Modulus *E*. Their probability distributions are given in Table 5.

Prof. G.I.N. Rozvany, phone: +36 (26) 362 592, e-mail: smo.rozvany@axelero.hu

Table 5. Random variables and distributions in example 5

Variable	Symbol	Mean	Standard deviation
Flange breadth	B	μ_B	$0.1\mu_B$
Flange thickness	D	μ_D	$0.1\mu_D$
Height of profile	H	μ_H	$0.1\mu_H$
Yield stress	F_S	400 Mpa	40 Mpa
Dead weight load	P_1	500,000 N	50,000 N
Variable load	P_2	600,000 N	60,000 N
Variable load	P_3	600,000 N	60,000 N
Initial deflection	F_0	30 mm	3 mm
Young's modulus	E	21,000 Mpa	2,100 Mpa

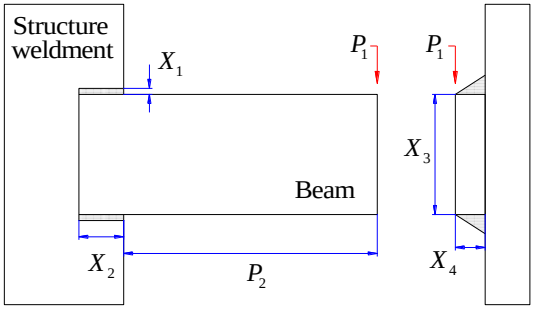

Fig. 7 A welded beam structure [27]

4.6 Example 6

Consider a welded beam design problem, as shown in Fig. 7. The objective function is to minimize the welding cost, and the probabilistic constraints involve mechanical properties of the welded beam such as the shear stress, bending stress, buckling, and free-end displacement. The design variables are the depth X_1 and length X_2 of the welding point, and the beam height X_3 and thickness X_4. The involved parameters include the following: free-end concentrated load P_1, beam length P_2, Young's Modulus P_3 and shear Modulus P_4 of the material, free-end allowable displacement P_5, allowable shear stress P_6, and allowable normal stress P_7. The above parameters are all independent random variables. The RBDO problem can be expressed as [27]:

Prof. G.I.N. Rozvany, phone: +36 (26) 362 592, e-mail: smo.rozvany@axelero.hu

$$\min_{\boldsymbol{\mu}_{\mathbf{X}}} f\left(\boldsymbol{\mu}_{\mathbf{X}}\right)=c_1\mu_{X_1}^2\mu_{X_2}+c_2\mu_{X_3}\mu_{X_4}\left(P_2+\mu_{X_2}\right)$$

$$\text{s.t. } \text{Prob}\left(g_j\left(\mathbf{X},\mathbf{P}\right)\ge 0\right)\ge \Phi\left(-\beta_j^{\text{t}}\right),\ \beta_j^{\text{t}}=3.0,\ j=1,2,...,5$$

$$g_1\left(\mathbf{X},\mathbf{P}\right)=\frac{\tau\left(\mathbf{X},\mathbf{P}\right)}{P_6}-1,\ g_2\left(\mathbf{X},\mathbf{P}\right)=\frac{\sigma\left(\mathbf{X},\mathbf{P}\right)}{P_7}-1,\ g_3\left(\mathbf{X}\right)=\frac{X_1}{X_4}-1,$$

$$g_4\left(\mathbf{X},\mathbf{P}\right)=\frac{\delta\left(\mathbf{X},\mathbf{P}\right)}{P_5}-1,\ g_5\left(\mathbf{X},\mathbf{P}\right)=1-\frac{P_c\left(\mathbf{X},\mathbf{P}\right)}{P_1},$$

$$3.175\text{mm}\le\mu_{X_1}\le 50.8\text{mm},\ \mu_{X_2}\le 254\text{mm},\ \mu_{X_3}\le 254\text{mm},\ \mu_{X_4}\le 50.8\text{mm},$$

$$\text{where } \tau\left(\mathbf{X},\mathbf{P}\right)=\sqrt{t\left(\mathbf{X},\mathbf{P}\right)^2+\frac{2t\left(\mathbf{X},\mathbf{P}\right)^2 tt\left(\mathbf{X},\mathbf{P}\right)^2}{2R\left(\mathbf{X}\right)}+tt\left(\mathbf{X},\mathbf{P}\right)^2},\ \ t\left(\mathbf{X},\mathbf{P}\right)=\frac{P_1}{\sqrt{2}X_1X_2},$$

$$tt\left(\mathbf{X},\mathbf{P}\right)=\frac{M\left(\mathbf{X},\mathbf{P}\right)R\left(\mathbf{X}\right)}{J\left(\mathbf{X}\right)},\ M\left(\mathbf{X},\mathbf{P}\right)=P_1\left(P_2+0.5X_2\right),\ \delta\left(\mathbf{X},\mathbf{P}\right)=\frac{4P_1P_2^3}{P_3X_3^3X_4},$$

$$R\left(\mathbf{X}\right)=0.5\sqrt{X_2^2+\left(X_1+X_3\right)^2},\ J\left(\mathbf{X}\right)=\sqrt{2}X_1X_2\left[\frac{X_2^2}{12}+\frac{\left(X_1+X_3\right)^2}{4}\right],\qquad(23)$$

$$\sigma\left(\mathbf{X},\mathbf{P}\right)=\frac{6P_1P_2}{X_3^2X_4},\ P_c\left(\mathbf{X},\mathbf{P}\right)=\frac{4.013X_3X_4^3\sqrt{P_3P_4}}{6P_2^2}\left(1-\frac{X_3}{4p_2}\sqrt{\frac{P_3}{P_4}}\right)$$

where the constants $c_1=6.74135\times10^{-5}$ and $c_2=2.93585\times10^{-5}$ represent the welding cost coefficients. And the probability distributions for the involved uncertain parameters are given in Table 6.

Table 6. Random variables and distributions in example 6

Variable	Symbol	Mean	Standard deviation
Welding point depth	X_1	μ_{X1}	0.4 mm
Welding point length	X_2	μ_{X2}	4.0 mm
Beam height	X_3	μ_{X3}	4.0 mm
Beam thickness	X_4	μ_{X4}	0.4 mm
Concentrated load	P_1	26,688 N	2,668.8 N
Beam length	P_2	3,556 mm	355.6 mm
Young's Modulus	P_3	20,685 Mpa	2,068.5 Mpa
Shear Modulus	P_4	82,740 Mpa	8,274.0 Mpa
Allowable displacement	P_5	6.35 mm	0.635 mm
Allowable shear stress	P_6	93.77 Mpa	9.377 Mpa
Allowable normal stress	P_7	206.85Mpa	20.685Mpa

4.7 Analysis of the results

The computational results for the above six numerical examples are presented in Tables 2, 7-11. A comprehensive analysis on the 30 situations leads to the following conclusions:

(1) Convergence. As indicated in Table 12, SORA and ISV converged in all 30 situations of the six examples, but for 11 situations SLM did not converge; nine of these failures were due to the involved uniform

Prof. G.I.N. Rozvany, phone: +36 (26) 362 592, e-mail: smo.rozvany@axelero.hu

probability distributions. The results indicate that SORA and the ISV method proposed here exhibit better convergence than SLM. In addition, for all converged situations, the ISV method obtained optimization results that are very close to those obtained from SORA and SLM, thereby indicating to some extent that the ISV method has a fine computational accuracy.

(2) Efficiency. As indicated by Fig. 8, overall, the SLM and ISV methods have higher computational efficiency than SORA. In the 19 situations for which SLM converged, the ISV method had higher efficiency for 14 ones of them, whereas SLM was more efficient for 5 ones. Thus, the ISV method generally has a slight advantage over SLM in terms of efficiency. Compared with SORA, the ISV method has a more significant advantage in terms of efficiency: in 29 ones out of 30 situations, the computational cost of the ISV method was less than that of SORA. Moreover, as the problem complexity increases (more constraints and parameters), the efficiency advantage of the ISV method becomes more obvious. For example, the efficiency of the ISV method was 3-5 times that of SORA in Example 6. In Example 5, the efficiency of the ISV method reached even 10-12 times that of SORA.

(3) Summing up the above two points, we can see that the ISV method not only inherits the good convergence property of SORA but also possesses the high computational efficiency of the approximation methods such as SLM. Therefore, the result analysis of the above numerical examples has demonstrated that the ISV method exhibits a stronger overall performance in terms of convergence and efficiency. This superior overall performance has a very good application potential for reliability design of many complex structures or products.

Table 7. Optimization results for numerical example 2

Distribution	Results	SORA	SLM	ISV
Y_1, Y_2, y, E: Normal	$\mathbf{d}^*$	2.239, 4.477	2.240, 4.477	2.230, 4.497
	f^*	10.026	10.026	10.025
	N_I	4	3	3
	N_F	489	67	79
	$\boldsymbol{\beta}$	3, 3.4	3, 3.5	3, 3.4
Y_1, Y_2, y, E: Lognormal	$\mathbf{d}^*$	2.213, 4.422	2.212, 4.423	2.200, 4.447
	f^*	9.784	9.784	9.783
	N_I	4	2	2
	N_F	432	47	48
	$\boldsymbol{\beta}$	3.0, 3.4	3.0, 3.3	3.0, 3.3
Y_1, Y_2, y, E: Uniform	$\mathbf{d}^*$	2.180, 4.361	---	2.166, 4.360
	f^*	9.508	---	9.446
	N_I	3	---	2
	N_F	378	---	50
	$\boldsymbol{\beta}$	3.0, 5.9	---	2.8, 6.5
Y_1, Y_2, y, E: Gumbel	$\mathbf{d}^*$	2.199, 4.340	2.199, 4.340	2.160, 4.351
	f^*	9.545	9.545	9.340
	N_I	4	3	3
	N_F	430	65	74
	$\boldsymbol{\beta}$	3.0, 3.0	3.0, 3.0	2.8, 2.7
Y_1: Normal Y_2: Lognormal y: Lognormal E: Gumbel	$\mathbf{d}^*$	2.226, 4.394	2.227, 4.391	2.202, 4.446
	f^*	9.780	9.780	9.792
	N_I	4	2	2
	N_F	488	51	49
	$\boldsymbol{\beta}$	3.0, 4.0	3.0, 3.8	3.0, 3.8

Prof. G.I.N. Rozvany, phone: +36 (26) 362 592, e-mail: smo.rozvany@axelero.hu

Table 8. Optimization results for numerical example 3

Distribution	Results	SORA	SLM	ISV
X_1, X_2: Normal	$\boldsymbol{\mu}_{\mathbf{x}}^*$	2.816, 3.277	2.817, 3.276	2.819, 3.279
	f^*	1.304	1.304	1.297
	N_I	3	4	2
	N_F	88	83	37
	$\boldsymbol{\beta}$	2.0, 21.9	2.0, 21.9	2.0, 21.9
X_1, X_2: Lognormal	$\boldsymbol{\mu}_{\mathbf{x}}^*$	2.814, 3.276	2.814, 3.276	2.819, 3.279
	f^*	1.309	1.309	1.296
	N_I	3	4	2
	N_F	86	81	37
	$\boldsymbol{\beta}$	2.0, 30.5	2.0, 30.5	2.0, 30.6
X_1, X_2: Uniform	$\boldsymbol{\mu}_{\mathbf{x}}^*$	2.818, 3.266	---	2.817, 3.270
	f^*	1.317	---	1.313
	N_I	3	---	2
	N_F	74	---	37
	$\boldsymbol{\beta}$	2.0, 205.0	---	2.0, 307.2
X_1, X_2: Gumbel	$\boldsymbol{\mu}_{\mathbf{x}}^*$	2.880, 3.129	2.785, 3.293	2.881, 3.130
	f^*	1.427	1.337	1.428
	N_I	5	5	27
	N_F	102	95	617
	$\boldsymbol{\beta}$	2.0, 54.2	2.0, 54.1	2.1, 54.2
X_1: Normal X_2: Uniform	$\boldsymbol{\mu}_{\mathbf{x}}^*$	2.802, 3.276	---	2.832, 3.265
	f^*	1.331	---	1.293
	N_I	3	---	2
	N_F	188	---	37
	$\boldsymbol{\beta}$	2.0, 41.0	---	1.9, 41.1

Prof. G.I.N. Rozvany, phone: +36 (26) 362 592, e-mail: smo.rozvany@axelero.hu

Table 9. Optimization results for numerical example 4

Distribution	Results	SORA	SLM	ISV
X_1~X_5: Normal	$\mathbf{d}^*, \boldsymbol{\mu}_{\mathbf{X}}^*$	17, 0.7, 3.58, 7.3 7.73, 3.36, 5.30	17, 0.7, 3.58, 7.3 7.75, 3.36, 5.30	17, 0.7, 3.58, 7.3 7.75, 3.36, 5.30
	f^*	3035.5	3036	3036.3
	N_I	2	2	2
	N_F	1358	375	326
	$\boldsymbol{\beta}$	6.7, 15.9, 64.1, 128.9, 3.1, 3.1, 3.0 80.1, 40.2, 3.0	6.7, 15.9, 63.3, 128.7, 3.1, 3.1, 3.0 80.1, 40.1, 3.0	6.7, 15.9, 63.3, 128.9, 3.1, 3.1, 3.0 80.1, 40.1, 3.0
X_1~X_5: Lognormal	$\mathbf{d}^*, \boldsymbol{\mu}_{\mathbf{X}}^*$	17, 0.7, 3.58, 7.3, 7.73, 3.36, 5.30	17, 0.7, 3.58, 7.3, 7.75, 3.36, 5.30	17, 0.7, 3.58, 7.3, 7.75, 3.36, 5.30
	f^*	3035.8	3036.2	3036.6
	N_I	2	2	2
	N_F	1372	375	330
	$\boldsymbol{\beta}$	6.9, 16.9, 51.5, 36.5, 3.0, 3.0, 3.0, 39.1, 12.5, 3.0	6.9, 16.9, 51.5, 36.5, 3.0, 3.0, 3.0, 39.1, 12.5, 3.0	6.9, 16.9, 51.5, 36.4, 3.0, 3.0, 3.0, 39.1, 12.5, 3.0
X_1~X_5: Uniform	$\mathbf{d}^*, \boldsymbol{\mu}_{\mathbf{X}}^*$	17, 0.7, 3.55, 7.3, 7.72, 3.35, 5.29	---	17, 0.7, 3.55, 7.3, 7.74, 3.35, 5.29
	f^*	3019.5	---	3017.4
	N_I	2	---	2
	N_F	2674	---	620
	$\boldsymbol{\beta}$	86.8, 188, 7, 1666, 3.0, 3.0, 3.0, 227.5, 354.6, 3.0	---	86.8, 188, 7, 1666, 3.0, 3.0, 3.0, 227.0, 354.6, 3.0
X_1~X_7: Gumbel	$\mathbf{d}^*, \boldsymbol{\mu}_{\mathbf{X}}^*$	17, 0.7, 3.6, 7.3 7.73, 3.35, 5.30	---	17, 0.7, 3.6, 7.3 7.75, 3.35, 5.30
	f^*	3039.8	---	3040.7
	N_I	2	---	2
	N_F	1724	---	337
	$\boldsymbol{\beta}$	46.4, 59.9, 57.3, 24.9 3.0, 3;0, 2.7, 39.0, 35.7, 3.0	---	46.4, 59.9, 55.5, 25.2, 3.3, 3.3, 2.7, 39.0, 39.4, 3.0
X_1: Normal X_2: Lognormal X_3, X_4: Uniform X_5: Gumbel	$\mathbf{d}^*, \boldsymbol{\mu}_{\mathbf{X}}^*$	17, 0.7, 3.58, 7.3, 7.72, 3.35, 5.30	---	17, 0.7, 3.58, 7.3, 7.74, 3.35, 5.30
	f^*	3030.3	---	3030.8
	N_I	2	---	2
	N_F	1371	---	431
	$\boldsymbol{\beta}$	6.7, 15.9, 33.0, 33.3, 3.0, 3.0, 3.0 80.1, 54.2, 3.0	---	6.7, 15.9, 33.0, 33.2, 2.9, 3.0, 3.0 80.1, 53.9, 3.0

Prof. G.I.N. Rozvany, phone: +36 (26) 362 592, e-mail: smo.rozvany@axelero.hu

Table 10. Optimization results for numerical example 5

Distribution	Results	SORA	SLM	ISV
	$\mu_B^*, \mu_D^*, \mu_H^*$	254.02, 13.72, 100.00	256.77, 13.57, 100.00	256.73, 13.48, 100.00
B, *D*, *H*, P_1, P_2, P_3,	f^*	3985.6	3984.5	3960.5
F_S, *E*, F_0: Normal	N_I	4	4	2
	N_F	602	81	51
	β	3.0	3.0	3.0
	$\mu_B^*, \mu_D^*, \mu_H^*$	251.72, 13.50, 100.00	253.66, 13.40, 100.00	254.40, 13.36, 100.00
B, *D*, *H*, P_1, P_2, P_3,	f^*	3898.6	3898.5	3897.5
F_S, *E*, F_0: Lognormal	N_I	4	4	2
	N_F	553	81	47
	β	3.0	3.0	3.0
	$\mu_B^*, \mu_D^*, \mu_H^*$	257.12, 13.57, 100.00	---	255.98, 13.44, 100.00
B, *D*, *H*, P_1, P_2, P_3,	f^*	3988.6	---	3940.1
F_S, *E*, F_0: Uniform	N_I	3	---	2
	N_F	465	---	49
	β	3.0	---	2.9
	$\mu_B^*, \mu_D^*, \mu_H^*$	244.96, 12.96, 100.00	244.37, 12.98, 100.00	246.39, 12.94, 100.00
B, *D*, *H*, P_1, P_2, P_3,	f^*	3673.8	3671	3687.1
F_S, *E*, F_0: Gumbel	N_I	4	4	2
	N_F	525	81	46
	β	3.0	3.0	3.0
	$\mu_B^*, \mu_D^*, \mu_H^*$	255.22, 13.68, 100.00	257.42, 13.54, 100.00	257.87, 13.54, 100.00
B,*D*,*H*: Normal	f^*	3990.7	3985.9	3991
P_1, P_2, P_3: Uniform	N_I	4	4	2
F_S, *E*: Lognormal	N_F	587	83	49
F_0: Gumbel	**β**	3.0	3.0	3.0

Prof. G.I.N. Rozvany, phone: +36 (26) 362 592, e-mail: smo.rozvany@axelero.hu

Table 11. Optimization results for numerical example 6

Distribution	Results	SORA	SLM	ISV
X_1~ X_4, P_1~P_7: Normal	$\boldsymbol{\mu}_{\mathbf{x}}^*$	10.07, 158.28, 210.89, 11.76	10.07, 158.30, 210.90, 11.76	10.00, 158.26, 210.89, 11.70
	f^*	4.8238	4.8238	4.7875
	N_I	3	4	3
	N_F	1532	391	323
	$\boldsymbol{\beta}$	3.0, 3.6, 3.0, 11.7, 8.8	3.0, 3.6, 3.0, 11.7, 8.8	3.0, 3.5, 3.0, 11.5, 8.7
X_1~ X_4, P_1~P_7: Lognormal	$\boldsymbol{\mu}_{\mathbf{x}}^*$	9.97, 158.28, 210.89, 11.68	9.97, 158.28, 210.89, 11.68	9.97, 158.26, 210.88, 11.68
	f^*	4.7774	4.7775	4.7756
	N_I	3	3	3
	N_F	1170	301	329
	$\boldsymbol{\beta}$	3.0, 3.6, 3.0, 9.7, 7.6	3.0, 3.6, 3.0, 9.7, 7.6	3.0, 3.6, 3.0, 9.6, 7.5
X_1~ X_4, P_1~P_7: Uniform	$\boldsymbol{\mu}_{\mathbf{x}}^*$	9.96, 158.23, 210.87, 11.30	---	9.87, 158.19, 210.85, 11.21
	f^*	4.6522	---	4.6021
	N_I	3	---	2
	N_F	1884	---	205
	$\boldsymbol{\beta}$	3.0, 4.1, 3.0, 288.7, 366.9	---	2.9, 3.9, 3.0, 388.7, 129.8
X_1~ X_4, P_1~P_7: Gumbel	$\boldsymbol{\mu}_{\mathbf{x}}^*$	10.17, 158.30, 210.91, 12.26	---	10.14, 158.30, 210.91, 12.05
	f^*	5.0068	---	4.9315
	N_I	3	---	6
	N_F	1783	---	607
	$\boldsymbol{\beta}$	3.0, 3.5, 3.0, 6.8, 6.3	---	3.0, 3.4, 2.8, 6.8, 6.1
X_1~ X_4: Uniform P_1, P_2, P_5: Lognormal P_3, P_4: Normal P_6, P_7: Gumbel	$\boldsymbol{\mu}_{\mathbf{x}}^*$	9.86, 158.22, 210.86, 11.20	---	9.91, 158.21, 210.86, 11.25
	f^*	4.5982	---	4.6253
	N_I	3	---	3
	N_F	1632	---	304
	$\boldsymbol{\beta}$	3.0, 3.4, 3.0 9.6, 3.5	---	3.04, 3.4, 3.0, 9.6, 7.6

Prof. G.I.N. Rozvany, phone: +36 (26) 362 592, e-mail: smo.rozvany@axelero.hu

Table 12. Comparison of convergence for 6 numerical examples

Method	SORA					SLM					ISV				
Case	1	2	3	4	5	1	2	3	4	5	1	2	3	4	5
Example 1	√	√	√	√	√	√	√	×	√	√	√	√	√	√	√
Example 2	√	√	√	√	√	√	√	×	√	√	√	√	√	√	√
Example 3	√	√	√	√	√	√	√	×	√	×	√	√	√	√	√
Example 4	√	√	√	√	√	√	√	×	×	×	√	√	√	√	√
Example 5	√	√	√	√	√	√	√	×	√	√	√	√	√	√	√
Example 6	√	√	√	√	√	√	√	×	×	×	√	√	√	√	√

√: Convergence; ×: Divergence.

Prof. G.I.N. Rozvany, phone: +36 (26) 362 592, e-mail: smo.rozvany@axelero.hu

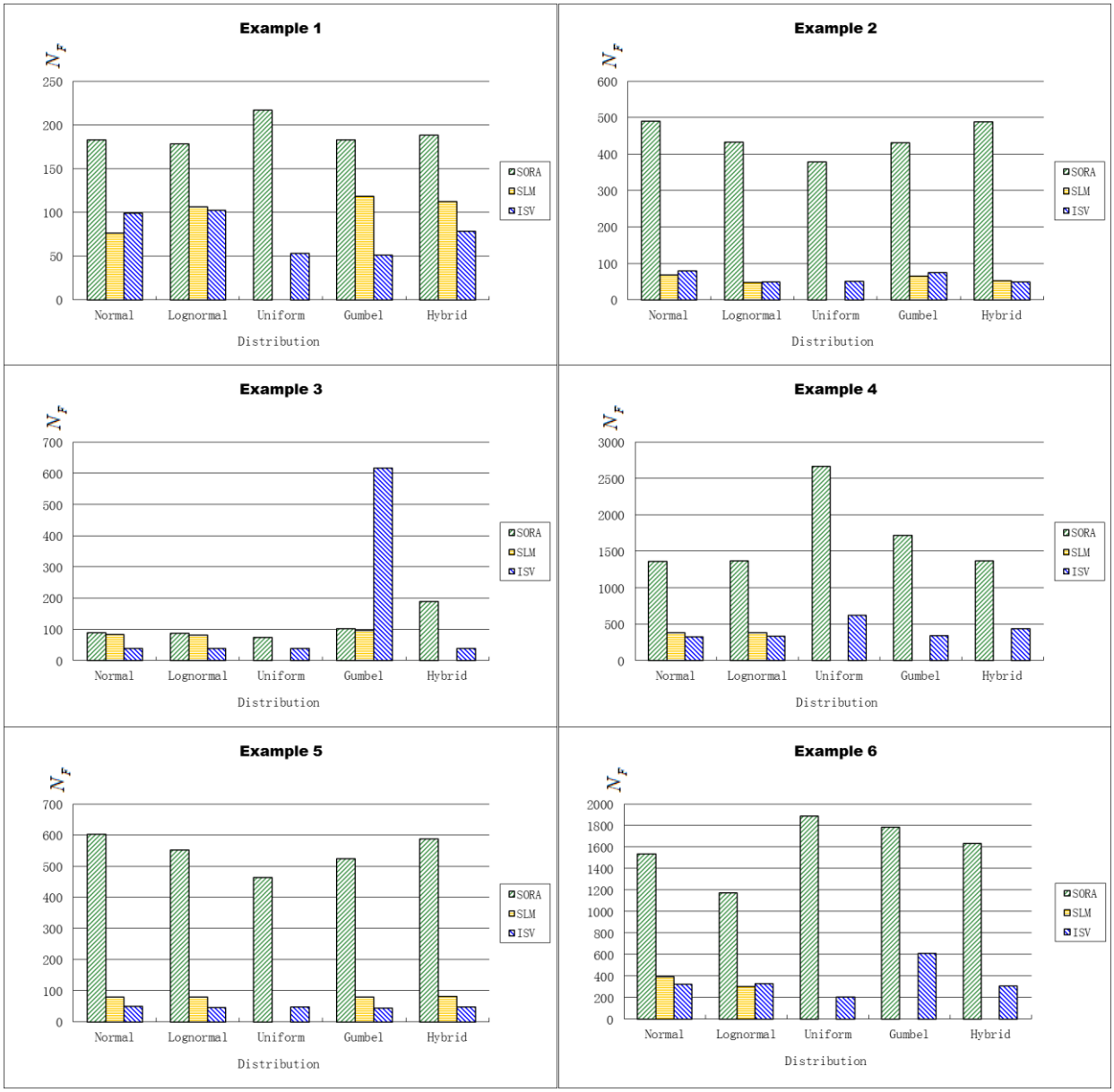

Fig. 8 Comparison of computational cost for 6 numerical examples

5 Engineering applications

5.1 Electronic packaging design for a smart watch

The wearable electronic device is generally highly integrated, which is required to satisfy some specific requirements in terms of mechanical, thermal and electrical performances using appropriate electronic packaging design. A smart watch as shown in Fig. 9 is considered in this problem. The thickness T^{m} on the midsection is required to minimize to satisfy the wearing comfort. Therefore, it is defined as the RBDO objective function. The smart watch should work reliably in some extreme conditions with hard impact and high temperature environment. In the hard impact environment, three identical steel balls are used to hit against the surface of the display in three different mark points, respectively. To ensure the display quality, the maximal stress in each point, $\Gamma_i^{\mathrm{N}}, i=1,2,3$, should be less than the yield strength $\Gamma^{\mathrm{Display}}$ of the material. In the high temperature environment, the operating temperature of the device is set as 50℃. The maximum temperature of Chip_1 and

Prof. G.I.N. Rozvany, phone: +36 (26) 362 592, e-mail: smo.rozvany@axelero.hu

Chip_2, T_1 and T_2, and the maximum stress Γ^{H} of the solder between display and main board are required to be less than the allowable values, T^{Chip} and Γ^{Solder}. The target reliability indexes for the constraints are $\beta_j \geq 2.0,\ j=1,2,3,4,5,6$. The thicknesses of the device housing, main board, bracket, display and lens, $X_i, i=1,2,...,5$, are treated as random design variables, which follow uniform distributions. The Young Modulus of the main board, display and lens, $P_i, i=1,2,3$, are random parameters. The power dissipation of Chip_1 and Chip_2, P_4 and P_5, are also treated as random parameters. The probability distributions for the design variables and parameters are given in Table 13. The RBDO problem is formulated as follows:

$$
\begin{aligned}
&\min_{\boldsymbol{\mu}_{\mathbf{X}}} T^{\mathrm{m}}\left(\boldsymbol{\mu}_{\mathbf{X}}\right)=\mu_{X_1}+\mu_{X_2}+\mu_{X_3}+\mu_{X_4}+\mu_{X_5}\\
&\text{s.t. } \operatorname{Prob}\left(g_j\left(\mathbf{X},\mathbf{P}\right)\geq 0\right)\geq \Phi\left(-\beta_j^{\mathrm{t}}\right),\ \beta_j^{\mathrm{t}}=3.0,\ j=1,2,3,4,5,6\\
&\quad g_1=\Gamma^{\mathrm{Display}}-\Gamma_1^{\mathrm{N}}\left(\mathbf{X},\mathbf{P}\right),\ g_2=\Gamma^{\mathrm{Display}}-\Gamma_2^{\mathrm{N}}\left(\mathbf{X},\mathbf{P}\right),\\
&\quad g_3=\Gamma^{\mathrm{Display}}-\Gamma_3^{\mathrm{N}}\left(\mathbf{X},\mathbf{P}\right),\ g_4=\Gamma^{\mathrm{Solder}}-\Gamma^{\mathrm{H}}\left(\mathbf{X},\mathbf{P}\right),\\
&\quad g_5=T^{\mathrm{Chip}}-T_1\left(\mathbf{X},\mathbf{P}\right),\ g_6=T^{\mathrm{Chip}}-T_2\left(\mathbf{X},\mathbf{P}\right),\\
&\quad \Gamma^{\mathrm{OLED}}=82.0\ \mathrm{Mpa},\ \Gamma^{\mathrm{Solder}}=62.8\ \mathrm{MPa},\ T^{\mathrm{Chip}}=90.0\ ^{\circ}\mathrm{C}\\
&\quad 1.0\mathrm{mm}\leq\mu_{X_i}\leq 2.0\mathrm{mm},\ i=1,2,3,4,5
\end{aligned}
\tag{25}
$$

The FEM models are established for all the performance functions as shown in Fig. 10, which are all implicit and time-consuming computational models. To realize the parameterization and also improve the optimization efficiency, a second-order polynomial response surface is created for each performance function by using 65 FEM samples, as shown in Table 14. The three methods, SORA, ISV and SLM, are all used to solve this problem with the same initial point $\boldsymbol{\mu}_{\mathbf{X}}^{\mathrm{initial}}=[1.50,1.00,1.50,1.40,1.20]$, and the results are provided in Table 15. Firstly, it can be seen that all reliability requirements of the smart watch are satisfied and the thickness of the device is reduced from 6.60mm to 6.29mm. Secondly, the optimal objective function values for SORA and ISV are 6.28mm and 6.29mm, respectively, which behaves only a small difference of 0.16%. It indicates that these two methods have a comparative accuracy for this problem. Thirdly, there is no result of SLM provided here, which is due to the fact that SLM is not convergent for this problem. Finally, SORA and ISV both require only a few iterations to reach an optimum. However, the total performance functional evaluations for SORA are 724, while it is only 381 for ISV. Therefore, ISV works more computationally efficient than SORA for this engineering application.

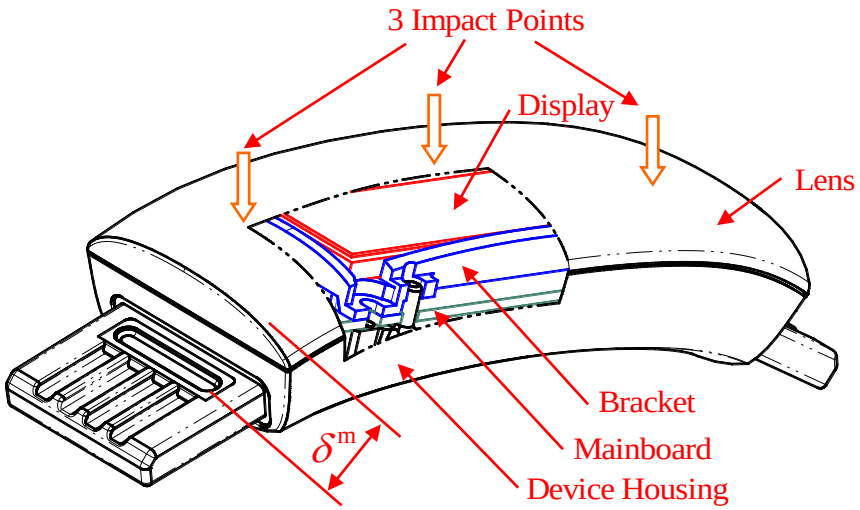

Fig.9 A smart watch

Prof. G.I.N. Rozvany, phone: +36 (26) 362 592, e-mail: smo.rozvany@axelero.hu

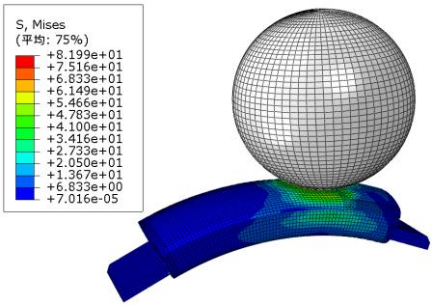

(a) Point 1 in hard impact (g_1)

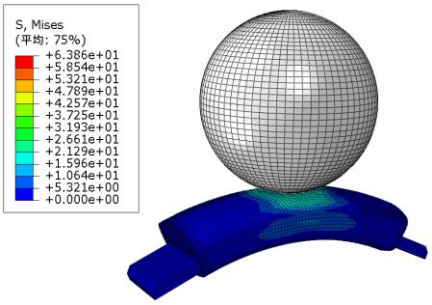

(b) Point 2 in hard impact (g_2)

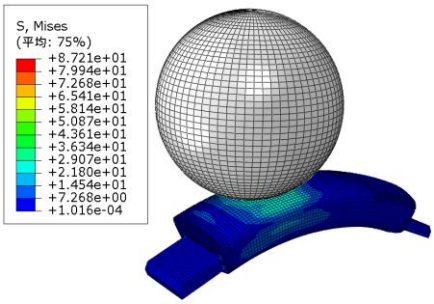

(c) Point 3 in hard impact (g_3)

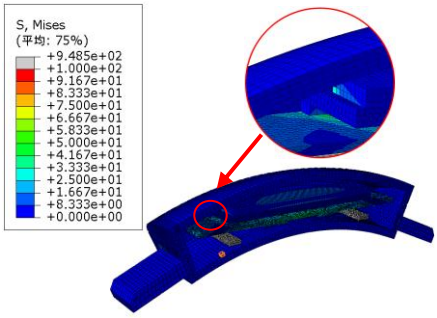

(d) Solder stress in high temperature (g_4)

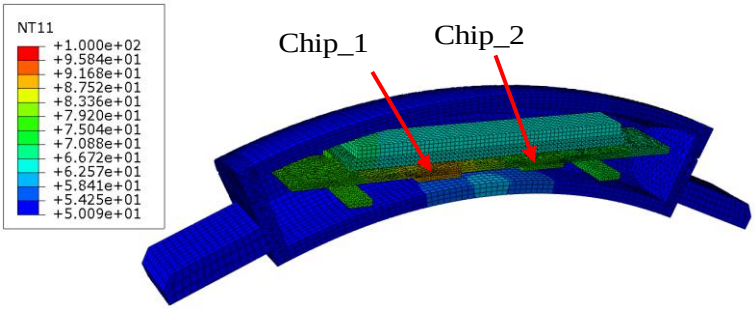

(e) Chip temperature in high temperature (g_5 , g_6)

Fig.10 Simulation models for the smart watch problem

Prof. G.I.N. Rozvany, phone: +36 (26) 362 592, e-mail: smo.rozvany@axelero.hu

Table 13. Random variables and distributions in engineering application 1

Variable	Symbol	Mean	Standard deviation	Distribution type
Device housing thickness	X_1	μ_{X1}	0.03 mm	Uniform
Main board thickness	X_2	μ_{X2}	0.03 mm	Uniform
Bracket thickness	X_3	μ_{X3}	0.03 mm	Uniform
Display thickness	X_4	μ_{X4}	0.03 mm	Uniform
Lens thickness	X_5	μ_{X5}	0.03 mm	Uniform
Main board Young's Modulus	P_1	11,000 Mpa	200 Mpa	Normal
Display Young's Modulus	P_2	23,000 Mpa	400 Mpa	Normal
Lens Young's Modulus	P_3	2,480 Mpa	100 Mpa	Normal
Chip_1 power dissipation	P_4	0.15 W	0.02 W	Normal
Chip_2 power dissipation	P_5	0.15 W	0.02 W	Normal

Table 14. Response surfaces for the performance functions in engineering application 1

Performance function	Response surface
$g_1 = \Gamma^{\mathrm{OLED}} - \Gamma_1^{\mathrm{N}}(\mathbf{X},\mathbf{P})$	$\Gamma_1^{\mathrm{N}}(\mathbf{X},\mathbf{P}) = 10^{-6}\left(0.001848P_2^2 - 0.3688P_2P_3 + 973.18P_2 + 1.609P_3^2\right)$ $-30.19X_1^2 + 1.133X_1X_3 + 33.10X_1X_4 + 1.313X_1X_5 + 0.4128X_3^2$ $-3.7317X_3X_4 - 0.26871X_3X_5 - 56.55X_4^2 + 65.54X_4X_5 - 55.32X_5^2 + 129.86$
$g_2 = \Gamma^{\mathrm{OLED}} - \Gamma_2^{\mathrm{N}}(\mathbf{X},\mathbf{P})$	$\Gamma_2^{\mathrm{N}}(\mathbf{X},\mathbf{P}) = 10^{-6}\left(-0.03509P_2^2 + 0.1813P_2P_3 + 1277P_2 - 1.461P_3^2\right)$ $-35.80X_1^2 + 6.112X_1X_3 + 32.86X_1X_4 + 2.891X_1X_5 - 6.809X_3^2$ $+4.303X_3X_4 + 9.209X_3X_5 - 63.71X_4^2 + 67.43X_4X_5 - 64.37X_5^2 + 135.2$
$g_3 = \Gamma^{\mathrm{OLED}} - \Gamma_3^{\mathrm{N}}(\mathbf{X},\mathbf{P})$	$\Gamma_3^{\mathrm{N}}(\mathbf{X},\mathbf{P}) = 10^{-6}\left(0.03054P_2^2 - 0.95P_2P_3 + 802.6P_2 + 4.645P_3^2\right)$ $-28.19X_1^2 + 4.188X_1X_3 + 28.63X_1X_4 + 0.2030X_1X_5 + 9.152X_3^2$ $-16.12X_3X_4 - 15.75X_3X_5 - 42.17X_4^2 + 62.61X_4X_5 - 36.32X_5^2 + 119.5$
$g_4 = \Gamma^{\mathrm{Solder}} - \Gamma^{\mathrm{H}}(\mathbf{X},\mathbf{P})$	$\Gamma^{\mathrm{H}}(\mathbf{X},\mathbf{P}) = 0.0000002578P_1^2 - 0.00002501P_1X_2 - 0.9103X_1^2 + 0.02502X_1X_2$ $+0.6950X_1X_3 + 0.1007X_2^2 + 0.0125X_2X_3 - 2.372X_3^2 + 37.54$
$g_5 = T^{\mathrm{Chip}} - T_1(\mathbf{X},\mathbf{P})$	$T_1(\mathbf{X},\mathbf{P}) = 0.5473X_1^2 - 2.932X_1X_2 - 0.3207X_1X_3 + 5.589X_2^2 - 2.970X_2X_3$ $-1.206X_3^2 + 71.85P_4 + 72.81P_5 + 299.3P_4P_5 + 62.05$
$g_6 = T^{\mathrm{Chip}} - T_2(\mathbf{X},\mathbf{P})$	$T_2(\mathbf{X},\mathbf{P}) = 0.5448X_1^2 - 2.923X_1X_2 - 0.3219X_1X_3 + 5.569X_2^2 - 2.973X_2X_3$ $-1.204X_3^2 + 61.10P_4 + 96.78P_5 + 255.2P_4P_5 + 61.11$

Prof. G.I.N. Rozvany, phone: +36 (26) 362 592, e-mail: smo.rozvany@axelero.hu

Table 15. Optimization results for engineering application 1

Results	Symbol	SORA	ISV
Design optimum	$\boldsymbol{\mu}_{\mathbf{X}}^{*}$	(1.00mm, 0.80 mm,1.92 mm, 1.20 mm, 1.36 mm)	(1.00mm, 0.80mm, 1.93mm, 1.20mm, 1.36mm)
Objective optimum	$T^{\mathrm{m}*}$	6.28 mm	6.29 mm
Reliability index at the optimum	$\boldsymbol{\beta}^{*}$	4.9, 2.0, 4.9, 2.0, 4.8, 4.5	4.9, 2.0, 4.9, 2.0, 4.5, 4.5
Iteration numbers	N_{I}	3	4
Performance functional evaluations	N_{F}	724	381

5.2 An automobile crashworthiness design

Lightweight design of automobile offers a promising way to improve the vehicle power performance, while it may also lead to the degradation of vehicle crashworthiness to some extent. Therefore, it seems useful to obtain a trade-off between the two aspects using the RBDO method. A vehicle model [40] as shown in Fig. 11 is considered. The design objective is to minimize the total mass *M* of the five key parts of the vehicle, namely, the crash box inner and outer plates, the front longitudinal beam inner and outer plates, the frontal bumper. The constraints are the vehicle crashworthiness requirements. The low-speed offset collision analysis at 15km/h and the high-speed frontal collision analysis at 56.4km/h are both conducted for the vehicle in this example. In the low-speed collision, the protection of the vehicle body is the priority because passenger safety is barely threatened in this case. The deformation of the front longitudinal beam can be described using the absorbed energy *E* in the collision, which should be less than an allowable value E_0 to guarantee the low-speed crashworthiness. In the high-speed collision, the damage to the passenger is required to be controlled and a safety space should be ensured. Therefore, the mean integration acceleration of the left backseat, $\bar{a}$, and the intrusion quantities of the upper and lower mark points, I^{H} and I^{L}, are required to be less than the given allowable values $\bar{a}_0$, I_0^{H} and I_0^{L} respectively. The target reliability indexes for the four constraints are set as $\beta_j \geq 2.0, j = 1,2,3,4$. The thickness X_1 of the front bumper, the thicknesses X_2 and X_3 of the crash box inner and outer plates, the thicknesses X_4 and X_5 of the front longitudinal beam inner and outer plates are treated as uncertain design variables, as shown in Table 16. The RBDO problem is then formulated as follows:

Prof. G.I.N. Rozvany, phone: +36 (26) 362 592, e-mail: smo.rozvany@axelero.hu

$$
\begin{aligned}
&\min_{\boldsymbol{\mu}_{\mathbf{X}}} M\left(\boldsymbol{\mu}_{\mathbf{X}}\right)=2.088\mu_{X_1}+0.404\mu_{X_2}+0.22\mu_{X_3}+1.2\mu_{X_4}+0.887\mu_{X_5}\\
&\text{s.t. } \operatorname{Prob}\left(g_j\left(\mathbf{X}\right)\geq 0\right)\geq \Phi\left(-\beta_j^{\mathrm{t}}\right),\ \beta_j^{\mathrm{t}}=2.0,\ j=1,2,3,4\\
&\quad g_1=E_0-E\left(\mathbf{X}\right),\ g_2=\bar{a}_0-\bar{a}\left(\mathbf{X}\right),\\
&\quad g_3=I_0^{\mathrm{H}}-I^{\mathrm{H}}\left(\mathbf{X}\right),\ g_4=I_0^{\mathrm{L}}-I^{\mathrm{L}}\left(\mathbf{X}\right)\\
&\quad \bar{a}_0=40\ \mathrm{g},\ E_0=300\ \mathrm{J},\ I_0^{\mathrm{H}}=270\ \mathrm{mm},\ I_0^{\mathrm{L}}=180\ \mathrm{mm}\\
&\quad 2.0\mathrm{mm}\leq\mu_{X_1}\leq 3.0\mathrm{mm},\ 1.0\mathrm{mm}\leq\mu_{X_2}\leq 3.0\mathrm{mm},\ 1.0\mathrm{mm}\leq\mu_{X_3}\leq 2.5\mathrm{mm},\\
&\quad 1.5\mathrm{mm}\leq\mu_{X_4}\leq 3.0\mathrm{mm},\ 1.0\mathrm{mm}\leq\mu_{X_5}\leq 3.0\mathrm{mm}
\end{aligned}
\tag{24}
$$

The FEM models are established for all the performance functions, as shown in Fig. 12. The response surfaces for the performance functions are also created based on 65 FEM samples, as shown in Table 17. In this application, SORA, ISV and SLM methods are all used to solve the above RBDO problem with a same initial point $\boldsymbol{\mu}_{\mathbf{X}}^{\text{initial}}=\left[2.20, 2.20, 2.20, 2.20, 2.20\right]$. For this initial point, the actual reliability indexes of the four constrains are $\boldsymbol{\beta}^{\text{Initial}}=\left[0.0,\ 4.5,\ 0.0,\ 4.5\right]$. Obviously, the first and third constrains cannot reach the target reliabilities. After RBDO analysis, the obtained optimal designs through the three methods are very close as shown in Table 18. From the optimization results, it can be found that the thicknesses of the five parts have been redistributed and the reliability requirements for all the constraints are then satisfied. What's more, the lightweight design is improved slightly since the mass is reduced from 10.56 kg to 10.44 kg. In this application, the total performance functional evaluations for SORA, ISV and SLM are 452, 151 and 136, respectively, which indicates that ISV and SLM have obviously higher computational efficiency than SORA for this problem.

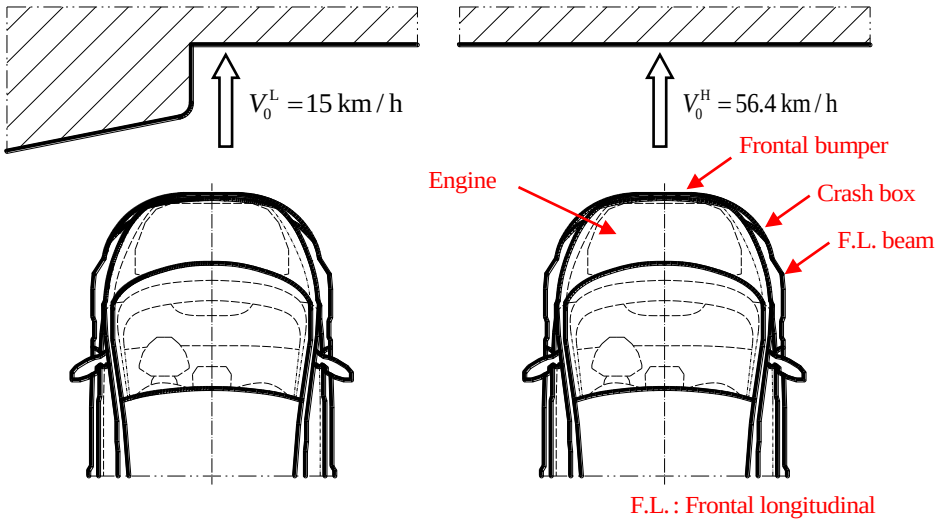

(a) Low-speed offset collision (g_1) (b) High-speed frontal collision (g_2 , g_3 , g_4)

Fig.11 Configurations of vehicle collision

Prof. G.I.N. Rozvany, phone: +36 (26) 362 592, e-mail: smo.rozvany@axelero.hu

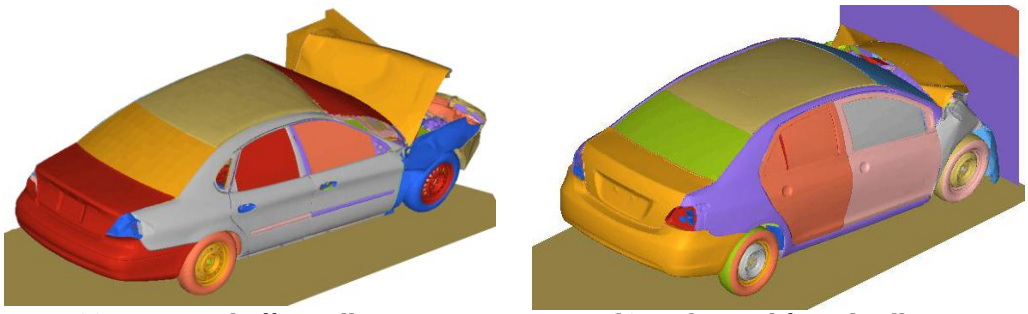

(a) Low-speed offset collision (b) High-speed frontal collision

Fig.12 Simulation models for the vehicle crashworthiness problem

Table 16. Random variables and distributions in engineering application 2

Variable	Symbol	Mean	Standard deviation	Distribution type
Frontal bumper thickness	X_1	μ_{X1}	0.05 mm	Normal
Crash box inner plate thickness	X_2	μ_{X2}	0.05 mm	Normal
Crash box outer plate thickness	X_3	μ_{X3}	0.05 mm	Normal
F.L. beam inner plate thickness	X_4	μ_{X4}	0.05 mm	Normal
F.L. beam outer plate thickness	X_5	μ_{X5}	0.05 mm	Normal

Prof. G.I.N. Rozvany, phone: +36 (26) 362 592, e-mail: smo.rozvany@axelero.hu

Table 17. Response surfaces for performance functions in engineering application 2

Performance function	Response surface
$g_1 = E_0 - E(\mathbf{X})$	$E(\mathbf{X}) = 109.428X_1 + 446.816X_2 + 292.161X_3 - 783.119X_4 - 1455.022X_5 - 78.912X_1X_2 - 179.822X_1X_3 + 55.735X_1X_4 + 68.927X_2X_3 + 97.546X_1X_5 - 99.046X_2X_4 - 88.414X_2X_5 - 35.461X_3X_4 + 52.259X_3X_5 + 185.717X_4X_5 + 14.85X_2^2 + 134.994X_4^2 + 275.308X_5^2 + 12779.336$
$g_2 = \bar{a}_0 - \bar{a}(\mathbf{X})$	$\bar{a}(\mathbf{X}) = 9.449X_2 - 1.832X_1 + 11.69X_3 + 10.636X_4 + 6.679X_5 - 1.232X_1X_2 - 1.329X_1X_4 + 1.106X_2X_3 - 0.914X_1X_5 - 1.313X_2X_5 - 3.759X_3X_4 - 1.1978X_3X_5 + 1.225X_1^2 - 2.366X_2^2 - 1.353X_3^2 - 0.906X_4^2 + 16.596$
$g_3 = I_0^{\mathrm{H}} - I^{\mathrm{H}}(\mathbf{X})$	$I^{\mathrm{H}}(\mathbf{X}) = 37.824X_1^2 + 12.634X_1X_2 - 21.495X_1X_3 - 20.773X_1X_5 - 135.479X_1 + 25.779X_2^2 - 15.08X_2X_4 + 8.781X_2X_5 - 123.145X_2 + 29.194X_3^2 + 7.606X_3X_4 - 65.554X_3 + 31.565X_4^2 - 15.874X_4X_5 - 93.243X_4 - 14.968X_5^2 + 106.945X_5 + 643.436$
$g_4 = I_0^{\mathrm{L}} - I^{\mathrm{L}}(\mathbf{X})$	$I^{\mathrm{L}}(\mathbf{X}) = 51.820X_1 - 9.242X_2 + 8.394X_3 - 79.998X_4 - 64.932X_5 - 5.156X_1X_2 + 6.211X_2X_3 + 14.747X_1X_5 - 5.878X_2X_4 - 9.894X_2X_5 - 8.811X_3X_4 - 2.477X_3X_5 + 7.152X_4X_5 - 15.196X_1^2 + 6.761X_2^2 + 20.438X_4^2 + 7.471X_5^2 + 275.327$

Table 18. Optimization results for engineering application 2

Results	Symbol	SORA	ISV	SLM
Design optimum	$\boldsymbol{\mu}_{\mathbf{X}}^*$	(2.31mm, 2.03mm, 1.63mm, 2.12mm, 2.12mm	(2.31mm, 2.04mm, 1.68mm, 2.11mm, 2.11mm)	(2.31mm, 2.03mm, 1.63mm, 2.12mm, 2.12mm)
Objective optimum	M^*	10.44 kg	10.44 kg	10.44 kg
Reliability index at the optimum	$\boldsymbol{\beta}^*$	2.0, 3.8, 2.0, 4.1	2.0, 2.7, 2.0, 4.1	2.0, 3.8, 2.0, 4.1
Iteration numbers	N_{I}	4	7	6
Performance functional evaluations	N_{F}	452	151	136

6 Conclusions

This paper proposed an ISV-based RBDO decoupling method that performs well in terms of both efficiency and convergence. The innovations of the proposed ISV method are that it uses a new incremental shifting strategy to ensure convergence in the iteration process and that it includes a new shifting vector computation method to avoid solving an optimization problem in the reliability analysis, which ensures high-efficiency RBDO solution. Through analyzing 30 different situations of six numerical examples as well as two practical applications, it was found that the ISV method possesses not only the similar convergence property of SORA but also the high

computational efficiency such as SLM. Also, the computational results can validate to some extent that the accuracy of the ISV method is guaranteed. Thus the proposed ISV method has a good application potential in reliability design of many complex structures or products. In the future, the ISV method can be expanded into reliability design for problems involving multidisciplinary analysis and problems including probabilistic and non-probabilistic hybrid uncertainties.

ACKNOWLEDGEMENT

This study is supported by the National Science Foundation for Excellent Young Scholars (51222502), the Key Project of Chinese National Programs for Fundamental Research and Development (2012AA111710), and the National Science Foundation of China (11172096).

Reference

[1] Enevoldsen, I., and Sørensen, J. D., 1994, "Reliability-Based Optimization in Structural Engineering," Struct. Safety, **15**(3), pp. 169–196.

[2] Chandu, S., and Grandhi, R., 1995, "General Purpose Procedure for Reliability Based Structural Optimization under Parametric Uncertainties," Adv. Eng. Softw., **23**(1), pp. 7-14.

[3] Kuschel, N., and Rackwitz, R., 1997, "Two Basic Problems in Reliability-Based Structural Optimization," Math. Meth. Oper. Res., **46**(3), pp. 309-333.

[4] Kirjner-Neto, C., Polak, E.,and Der Kiureghian, A., 1998, "An Outer Approximations Approach to Reliability-Based Optimal Design of Structures," J. Optim. Theory Appl., **98**(1), pp. 1-16.

[5] Tu, J., Choi, K. K., and Park, Y. H., 1999, "A New Study on Reliability-Based Design Optimization," AMSE J. Mech. Des. **121**(4), pp. 557-564.

[6] Royset, J. O., Der Kiureghian, A., and Polak, E., 2001, "Reliability-based Optimal Design of Series Structural Systems," ASCE J. Eng. Mech., **127**(6), pp. 607–614.

[7] Li, G., and Cheng, G. D., 2001, "Optimal Decision for the Target Value of Performance Based Structural System Reliability," Struct. Multidisc. Optim., **22**(4): 261-267.

[8] Youn, B. D., and Choi, K. K., 2004, "A New Response Surface Methodology for Reliability-Based Design Optimization," Comput. Struct., **82**(2-3). pp. 241-256.

[9] Kim, C., and Choi, K. K., 2008, "Reliability-Based Design Optimization Using Response Surface Method With Prediction Interval Estimation," ASME J. Mech. Des., **130**(12), pp. 1401-1412.

[10] Basudhar, A., and Missoum, S., 2008, "Adaptive Explicit Decision Functions for Probabilistic Design and Optimization Using Support Vector Machines", Comput. Struct., **86**(19), pp. 1904–1917.

[11] Shan, S. Q. and Wang, G., 2009, "Reliable Space Pursuing for Reliability-Based Design Optimization with Black-box Performance Function," Chinese J. Mech. Eng., **22**(1), pp. 27-35.

[12] Zhuang, X. T., and Pan, R., 2012, "A Sequential Sampling Strategy to Improve Reliability-Based Design Optimization with Implicit Constraint Functions," ASME J. Mech. Des., **134**(2), pp. 1002-1012.

[13] Wu, Y.T., and Wang, W., 1998, "Efficient Probabilistic Design by Converting Reliability Constraints to Approximately Equivalent Deterministic Constraints," J. Integr. Des. Process. Sci., 2(4), pp. 13–21.

[14] Du, X. P., and Chen, W., 2004, "Sequential Optimization and Reliability Assessment Method for Efficient Arobabilistic Design," ASME J. Mech. Des., **126**(2), pp. 225–233.

[15] Liang, J., Mourelatos Z. P., and Tu, J., 2004, "A Single-Loop Method for Reliability-based design optimization," Proceedings of ASME Design Engineering Technical Conferences, Salt Lake City, UT.

[16] Cheng G. D., Xu, L., Jiang, L., 2006, "A Sequential Approximate Programming Strategy for Reliability-Based Structural Optimization," Comput. Struct., **84**(21), pp. 1353–1367.

[17] Shan, S., and Wang, G., 2008, "Reliable design space and complete single-loop reliability-based design optimization," Rel. Eng. Sys. Safety, **93**(8), pp. 1218-1230.

Prof. G.I.N. Rozvany, phone: +36 (26) 362 592, e-mail: smo.rozvany@axelero.hu

[18] Agarwal，H., Gano, S. E., and Pérez, V. M., 2009, "Homotopy Methods for Constraint Relaxation in Unilevel Reliability Based Design Optimization," Eng. Optim., **41**(6), PP. 593-607.

[19] Huang, H. Z., Zhang, X. D., and Liu, Y., 2012, "Enhanced Sequential Optimization and Reliability Assessment for Reliability-Based Design Optimization," J. Mech. Sci. Tec., **26**(7). pp. 2039~2043.

[20] Chen, Z. Z., Qiu, H. B., and Gao, L., 2013, "An Optimal Shifting Vector Approach for Efficient Probabilistic Design," Struct. Multidisc. Optim. **47**(6), pp. 905–920.

[21] O. Madsen, H., and Friis Hansen, P., 1992, "A Comparison of Some Algorithms for Reliability-Based Structural Optimization and Sensitivity Analysis," In: Rackwitz R, Thoft-Christensen P (eds) Proceedings of the 4th IFIP WG 7.5 Conference, Munich. Springer-Verlag, Berlin, pp. 443–451.

[22] Torng, T. Y., and Yang, R. J., 1993, "An Advanced Reliability-Based Optimization Method for Robust Design Optimization Method," In: Spanos PD, Wu YT (eds) Probabilistic Structural Mechanics: Advances in Structural Reliability Methods. Springer, New-York, pp. 534–549.

[23] Chen, X., Hasselman, T. K., and Neill, D. J., 1997, "Reliability-Based Structural Design Optimization for Practical Applications," In: Proceedings of the 38th AIAA/ASME/ASCE/AHS/ASC Structures, Structural Dynamics, and material Conference, Kissimmee, AIAA-97-1403.

[24] Royset, J. O., Der Kiureghian, A., and Polak, E., 2001, "Reliability-Based Optimal Structural Design by the decoupling approach," Rel. Eng. Sys., 73(3), pp. 213–221.

[25] Kharmanda, G., Mohamed, A. and Lemaire, M., 2002, "Efficient reliability-based design optimization using a hybrid space with application to finite element analysis," Struct. Multidis. Optim., 24(3). pp. 233–245.

[26] Du, X. P., and Huang. B. Q., 2007, "Reliability-Based Design Optimization with Equality Constraints," Int. J. Numer. Methods Eng., **72**(11). 1314–1331.

[27] Cho, T. M., and Lee, B. C., 2010, "Reliability-Based Design Optimization Using Convex Approximations and Sequential Optimization and Reliability Assessment Method," J. Mech. Sci. Tec., **24**(2010), pp. 279-283.

[28] Hasofer, A. M., and Lind, N. C., 1974, "Exact and Invariant Second-Moment Code Format," J. Eng. Mech. Div., **100**(1), pp. 111–121.

[29] Rackwitz, R., and Fiessler, B., 1978, "Structural Reliability under Combined Random Load Sequences," Comput. Struct., **9**(5), pp. 489–494.

[30] Madsen, H. O., Krenk, S., and Lind, N. C., 1986, *Methods of structural safety*, Prentice Hall, Englewood Cliffs.

[31] Melchers, R. E., 1999, *Structural Reliability Analysis and Prediction*, John Wiley & Sons, Chichester.

[32] Reddy, M. V., Grandhi, R. V., and Hopkins, D. A., 1994,"Reliability-Based Structural Optimization: A Simplified Safety Index Approach," Comput. Struct., **53**(6), pp. 1407-1418.

[33] Tu J, K., Choi K, H., and Park, Y., 1999, "A New Study on Reliability-Based Design Optimization," AMSE J. Mech. Des., **121**(4), pp. 557-564.

[34] Wu. Y. , Millwater, H. A., and Cruse, T., 1990, "Advanced Probabilistic Structural Analysis Method for Implicit Performance Functions," AIAA J., **28**(9), pp. 1663-1669.

Prof. G.I.N. Rozvany, phone: +36 (26) 362 592, e-mail: smo.rozvany@axelero.hu

[35] Wu. Y., 1994, "Computational Methods for Efficient Structural Reliability and Reliability Sensitivity Analysis," AIAA J., **32**(8), pp. 1717-1723.

[36] Youn, B. D., Choi K. K., and Park, Y. H., 2003, "Hybrid Analysis Method for Reliability-Based Design Optimization,", ASME J. Mech. Des., **125**(2), pp. 221-232.

[37] Du, X. P., Sudjianto, A., and Chen, W., 2003, "An Integrated framework for Optimization under Uncertainty Using Inverse Reliability Strategy," DETC2003/DAC-48706, 2003 ASME International Design Engineering Technical Conferences and the Computers and Information in Engineering Conference, Chicago, Illinois.

[38] Burden, R. L. and Faires, J. D., 1985, *Numerical Analysis*, Prindle, Weber & Schmidt, Boston, MA.

[39] Roger, F., 2000, *Practical Methods of Optimization*, John Wiley & Sons Ltd., New York.

[40] Jiang, C., Deng, S. L., 2014, "Multi-objective Optimization and Design Considering Automotive High-speed and Low-speed Crashworthiness," Chinese J. Comput. Mech. 31(04), pp. 474 – 479.

Prof. G.I.N. Rozvany, phone: +36 (26) 362 592, e-mail: smo.rozvany@axelero.hu

Figure captions

Prof. G.I.N. Rozvany, phone: +36 (26) 362 592, e-mail: smo.rozvany@axelero.hu

Table captions

Prof. G.I.N. Rozvany, phone: +36 (26) 362 592, e-mail: smo.rozvany@axelero.hu

Summary of Revisions （Reviewer 1）

The authors appreciate very much the comments and suggestions from the reviewer. The suggestions are very helpful to improve the paper, and have been incorporated in the revised manuscript. Modifications have been made as follows:

1） It is suggested that the editorial improvement is necessary for maintaining the quality of the paper. Thus I recommend a minor revision with an editorial improvement through a proofreading by a native speaker or a very experienced language editor.

The paper has been carefully modified.

Summary of Revisions （Reviewer 2）

The authors appreciate very much the comments and suggestions from the reviewer. The suggestions are very helpful to improve the paper, and have been incorporated in the revised manuscript. Modifications have been made as follows:

1） I see that another reviewer also pointed out using G(U=0) and G(U_MPP). Through your examples you show that ISV might not introduce error. Since you are not providing a theoretical proof, it is good to introduce the sentence: "The results can validate to some extend that the accuracy of the ISV method is guaranteed." in the text.

This has been modified.

Summary of Revisions （Reviewer 3）

The authors appreciate very much the comments and suggestions from the reviewer. The suggestions are very helpful to improve the paper, and have been incorporated in the revised manuscript. Modifications have been made as follows:

1) The paper needs some editorial improvements before acceptance for publication.

This paper has been modified carefully.